

The Continuous Slope-Area Method for Computing Event Hydrographs



Scientific Investigations Report 2010-5241

Cover. Babocomari River in southern Arizona, looking downstream during a summer flow event (photograph by J.T. Cordova).

The Continuous Slope-Area Method for Computing Event Hydrographs

By Christopher F. Smith, Jeffrey T. Cordova, and Stephen M. Wiele

Scientific Investigations Report 2010–5241

U.S. Department of the Interior
U.S. Geological Survey

U.S. Department of the Interior
KEN SALAZAR, Secretary

U.S. Geological Survey
Marcia K. McNutt, Director

U.S. Geological Survey, Reston, Virginia: 2010

This report and any updates to it are available online at:
<http://pubs.usgs.gov/sir/2010/5241/>

For more information on the USGS—the Federal source for science about the Earth, its natural and living resources, natural hazards, and the environment:
World Wide Web: <http://www.usgs.gov/>
Telephone: 1-888-ASK-USGS

Any use of trade, product, or firm names in this publication is for descriptive purposes only and does not imply endorsement by the U.S. Government.

Although this report is in the public domain, it may contain copyrighted materials that are noted in the text. Permission to reproduce those items must be secured from the individual copyright owners.

Library of Congress Cataloging-in-Publication Data

Suggested citation:
Smith, C.F., Cordova, J.T., and Wiele, S.M., 2010, The continuous slope-area method for computing event hydrographs: U.S. Geological Survey Scientific Investigations Report 2010-5241, 37 p.

Contents

Abstract.....	1
Introduction.....	1
Purpose and Scope	1
Discharge Measurements Using the Slope-Area Method	2
The Slope-Area Computation Program	2
Sensitivity of Indirect Discharge Computations to Slope	2
The Continuous Slope-Area Method	3
Site Selection.....	3
Evaluation of Pressure-Transducer Data and Calculated Hydrographs	4
Comparison of Pressure-Transducer Peaks to Crest-Stage Gage Peaks.....	4
Stage-Discharge Relations	4
Hysteresis in the Stage-Discharge Relations	4
Evaluation of Channel Geometry	5
The Effect of Unsteadiness on Discharge Computation Accuracy.....	5
Study Site on the Babocomari River.....	5
Description of Channel Conditions along the Slope-Area Reach and Roughness Coefficient Selection.....	9
Application of the Continuous Slope-Area Method on the Babocomari River	11
Installation of Pressure Transducers	11
Collection and Reduction of Pressure-Transducer Data	12
Calculation of Hydrographs Using the Continuous Slope-Area Method.....	13
Batch-Processing Discharge Computations.....	13
Development of Stage-Discharge Relations	14
Major Flows on the Babocomari River 2002–2006	14
Flow of October 9, 2003	14
Channel Geometry	14
Evaluation of the High-Water Marks	16
Conventional Slope-Area Computation and Analysis.....	17
Evaluation of the Pressure-Transducer Data.....	18
Continuous Slope-Area Discharge Computations and Analysis	18
Rating Development	18
Summary of the October 2003 Event.....	19
The Flow Event of July 27, 2006	19
Changes in Channel Shape	19
Evaluation of the High-Water Marks	20
Slope-Area Computation and Analysis of High-Water Marks	20
Slope-Area Computation of Peak Discharge using PT Data and Analysis of PT Data	22
Evaluation of the Pressure-Transducer Data.....	23
Development of Stage-Discharge Relation.....	24
Transfer of the CSA Stage-Discharge Relation to the Babocomari River near Tombstone Streamflow-Gaging Station	24
Conclusions.....	26
References Cited.....	30

Figures

1.	Error in discharge calculated with equation 2, caused by errors in measured reach drop. The sample calculation shown is for a true drop in the reach of 0.5 ft.....	3
2.	Percent error in the St. Venant momentum equation as a result of neglecting the unsteady term as a function of change in velocity for three reach slopes.....	6
3.	Velocity and du/dQ as function of discharge for a trapezoidal channel with a bed width of 50 ft, slope of 0.001, and a Manning's n of 0.035. The bank width was specified as two times the depth.....	6
4.	Hydrograph computed with the Continuous Slope-Area method and the normalized unsteady term from the momentum equation ($du/dt)/(gS)$ during the July 27, 2006, event on the Babocomari River.....	7
5.	Histogram of the absolute value of the normalized unsteady term in equation 4 for the Babocomari River hydrograph shown in figure 4.....	7
6.	Map showing the study area on the Babocomari River.....	8
7.	View looking downstream from cross section 1. Note the dense grass where trees are sparse.....	9
8.	View looking upstream from cross section 4. Ash trees grow along the low-flow channel.....	9
9.	Views from cross section 1 looking upstream (left), downstream (center), and downstream (right).....	10
10.	Views from cross section 2 looking upstream (left), downstream (center), and downstream (right).....	10
11.	Views from cross section 3 looking upstream (left), downstream (center), and downstream (right).....	10
12.	Views from cross section 4 looking upstream (left), downstream (center), and downstream (right).....	11
13.	Installation of the crest-stage gage (left). The pressure transducer is clamped to the bottom of the crest-stage gage board (center and right).....	11
14.	Plan view of the cross sections and eight pressure transducers in the Babocomari River continuous-slope-area reach.....	12
15.	Pressure-transducer-pin elevations (dry with no flow).....	13
16.	Peak streamflows recorded on the Babocomari River during the study period, 2002–2006.....	14
17.	Stage hydrographs from the October 9, 2003, flow event on the Babocomari River.....	15
18.	Channel surveys in cross section 1 before and after the October 9, 2003, event. The blue dashed line shows the water-surface elevation at the peak discharge.....	16
19.	Channel surveys in cross section 2 before and after the October 9, 2003, event. The blue dashed line shows the water-surface elevation at the peak discharge.....	16
20.	Channel surveys in cross section 3 before and after the October 9, 2003, event. The blue dashed line shows the water-surface elevation at the peak discharge.....	17
21.	Channel surveys in cross section 4 before and after the October 9, 2003, event. The blue dashed line shows the water-surface elevation at the peak discharge.....	17
22.	Average left- and right-bank pressure-transducer-stage hydrographs during the October 9, 2003, event.....	18

23.	Discharge values computed with the average pressure-transducer and crest-stage gage data for the October 9, 2003, event	19
24.	Stage-discharge relation determined with discharges computed from the averaged pressure-transducer data and crest-stage gage data for the October 9, 2003, event.....	20
25.	July 27, 2006, stage hydrographs for six pressure transducers. Right-bank pressure transducers are indicated by R in the legend label; left-bank pressure transducers are indicated by L in the legend label; the number in the legend label corresponds to the cross-section number	21
26.	Right-bank pressure transducer in cross section 1 (PTR1) after the July 27, 2006, flow event.....	22
27.	View looking upstream from cross section 3 on the right bank after the July 27, 2006, event. The floodway is mostly clear of obstacles	22
28.	Channel surveys in cross section 1 before and after the July 27, 2006, event. The blue line shows the water-surface elevation at the peak discharge. At the peak discharge, the difference in cross-section areas is 2 percent	22
29.	Channel surveys in cross section 2 before and after the July 27, 2006, event. The blue line shows the water-surface elevation at the peak discharge. At the peak discharge, the difference in cross-section areas is 8 percent	23
30.	Channel surveys in cross section 3 before and after the July 27, 2006, event. The blue line shows the water-surface elevation at the peak discharge. At the peak discharge, the difference in cross-section areas is 0.5 percent	23
31.	Channel surveys in cross section 4 before and after the July 27, 2006, event. The blue line shows the water-surface elevation at the peak discharge. At the peak discharge, the difference in cross-section areas is 4 percent	24
32.	Debris pile near left bank in cross section 3 after the July 27, 2006, event	26
33.	Stage hydrographs of the four pressure transducers that were used to compute discharge for the July 27, 2006, event	27
34.	Stage values from the left-bank pressure transducer in cross section 1 and the corresponding discharge computed with stage data in X1-X4 during the July 27, 2006, event are shown as dots. All stage and discharges shown occurred prior to the rotation of the pressure transducers. The solid line is a cubic polynomial fitted to the stage-discharge relation	28
35.	Reach below the Babocamari River near the Tombstone stream gage was heavily vegetated prior to the July 27, 2006, event (left). Much of that vegetation was gone after the event (right). The rock in the right foreground of the left photograph is the same as the rock occupying the right lower quadrant of the right photograph	29
36.	Stage hydrographs from the Babocamari River near Tombstone gage and the left bank pressure transducer in cross section 1 (PTL1) during the July 27, 2006, event. Stages from the two sites were adjusted to coincide on the rising limb	29
37.	Stage-discharge relations before and after the July 27, 2006, event. The blue line represents conditions prior to the peak and included the effects of the dense vegetation. The red curve represents the condition after vegetation was scoured.....	30

Tables

1. Elevation difference between crest-stage and pressure-transducer datums (dry).....	13
2. Peak stages recorded by the crest-stage gages and by the pressure transducers during the October 9, 2003, event.....	15
3. Peak discharge for cross sections 1–4, based on average of left- and right- stage data from the pressure transducers and crest-stage gage from October 9, 2003, event.....	18
4. Water-surface elevations from surveyed high-water marks and pressure transducers from the July 27, 2006, event	25
5. Peak discharge computed using surveyed left-bank high-water marks for the July 27, 2006, event	25
6. Peak discharges computed using surveyed right-bank high-water marks for the July 27, 2006, event	25
7. Peak discharge computed with the left-bank pressure transducers for the July 27, 2006, event	25
8. Peak discharge computed with the right-bank pressure transducers for the July 27, 2006, event	26

Appendices

1. Stage data and computed discharge for five runoff events in the Babocomari River	31
2. Input files to the SAC program used in the continuous slope-area calculations of discharge for five events on the Babocomari River.....	35

Conversion Factors

Inch/Pound

Multiply	By	To obtain
	Length	
foot (ft)	0.3048	meter (m)
	Flow rate	
foot per second (fts/s)	0.3048	meter (m)

Temperature in degrees Celsius (°C) may be converted to degrees Fahrenheit (°F) as follows:
 $^{\circ}\text{F}=(1.8\times^{\circ}\text{C})+32$

Temperature in degrees Fahrenheit (°F) may be converted to degrees Celsius (°C) as follows:
 $^{\circ}\text{C}=(^{\circ}\text{F}-32)/1.8$

Vertical coordinate information is referenced to the insert datum name (and abbreviation) here for instance,

“North American Vertical Datum of 1988 (NAVD 88).”

Horizontal coordinate information is referenced to the insert datum name (and abbreviation) here for instance,

“North American Datum of 1983 (NAD 83).”

Altitude, as used in this report, refers to distance above the vertical datum.

This page intentionally left blank

The Continuous Slope-Area Method for Computing Event Hydrographs

By Christopher F. Smith, Jeffrey T. Cordova, Stephen M. Wiele

Abstract

The continuous slope-area (CSA) method expands the slope-area method of computing peak discharge to a complete flow event. Continuously recording pressure transducers installed at three or more cross sections provide water-surface slopes and stage during an event that can be used with cross-section surveys and estimates of channel roughness to compute a continuous discharge hydrograph. The CSA method has been made feasible by the availability of low-cost recording pressure transducers that provide a continuous record of stage. The CSA method was implemented on the Babocomari River in Arizona in 2002 to monitor streamflow in the channel reach by installing eight pressure transducers in four cross sections within the reach. Continuous discharge hydrographs were constructed from five streamflow events during 2002–2006. Results from this study indicate that the CSA method can be used to obtain continuous hydrographs and rating curves can be generated from streamflow events.

Introduction

The U.S. Geological Survey (USGS) operates about 7,500 stream gages throughout the Nation. The rating curves that relate stage to discharge at these gaging stations are formulated from periodic measurements of discharge at known stages. Stages are recorded at regular intervals, typically 15 min, and the discharge is computed from stage using the stage-discharge rating curve. A well-defined rating curve typically requires many discharge measurements at a range of discharges. Obtaining discharge measurements over a wide range of stage is not always possible as a result of remoteness of the streamflow-gaging stations, inaccessibility due to flooding, flashy events, or limited resources.

If a direct measurement of discharge is not obtained at a high flow, the USGS routinely uses slope-area method to estimate discharge (Dalrymple and Benson, 1967). A slope-area measurement is a discharge calculated using measured cross sections, estimations of channel roughness, and a water-surface slope derived from field evidence, such as

debris lines. The Manning equation, in which the slope is the energy slope, is used to calculate discharge.

The use of a water-surface slope derived from field evidence to calculate the discharge in slope-area measurements has two potential drawbacks. First, the high-water marks used to infer the water-surface slope may not be well defined and may not accurately represent the water-surface slope in the main part of the flow. Debris lines are subject to wave action, downslope creep, and diffusion by rainfall and gravity that produce inaccuracies or an apparent irregularity in the water-surface slope. Smaller peaks following a large event can add to the difficulty in identifying the relevant high-water marks. Bank roughness can generate real variability in the water-surface slope that poorly represents the slope near the center of the channel. The resulting scatter in the water surface that is used in the slope-area calculations can be a source of error. Second, the use of high-water marks allows only for the calculation of the peak discharge. The event hydrograph cannot be estimated from peak discharge calculations.

This report presents an extension of the slope-area method for obtaining peak discharges to a method for recording continuous time series stage at multiple cross sections, development of stage discharge relationships, and computation of discharge hydrographs for the slope-area reach. The method requires some foresight—slope-area reaches must be identified and instrumented prior to events—and, because the method depends on estimates of channel roughness and reaches with desirable properties for slope-area measurements may not be available, it cannot consistently achieve the level of accuracy characteristic of standard USGS stream gages with rating curves that are well defined by many direct discharge measurements. The method can produce more complete discharge records than would otherwise be possible, where the resources are not available to install and maintain stream gages or the required measurements are not possible due to logistical obstacles.

Purpose and Scope

The CSA method for computing hydrographs has been under development by the USGS Arizona Water Science Center Data Program since the summer of 2002. This report

2 The Continuous Slope-Area Method for Computing Event Hydrographs

describes the installation of crest-stage gages (CSG) with continuously recording pressure transducers (PT), data acquisition and analysis, and computed results from the Babocomari River continuous slope-area reach that was operated over a 5-yr period from 2002 to 2006, as well as the basics of the method and its implementation. Additional sections cover implementation of the method in the Babocomari River. Five significant flows occurred during the study period and the CSA method was used to determine a hydrograph for each of them; the application of the CSA method to two of these events is described in this report, and the stage data, computed discharges, and channel shape and roughness for all five events are available in appendices 1 and 2. Although the study lasted 5 years, the southeastern Arizona climate combined with drought conditions during the study period limited the total time of recorded flow to only about 9 hours. Thus, this report should be considered an initial application of the method and not a comprehensive techniques and methods manual. Other applications are ongoing (for example, Stewart and others, 2008) and will aid in refining field methods and the analysis of stage records.

Discharge Measurements Using the Slope-Area Method

A slope-area discharge measurement uses channel surveys, estimates of water-surface slopes, and estimates of channel roughness to calculate peak discharge. Benson and Dalrymple (1967) and Dalrymple and Benson (1967) explain the practical and theoretical components of slope-area discharge measurements. Channel geometry of the reach is important in producing accurate slope-area computations of discharge. Large changes in the shape of the channel along a reach, for example, should be avoided due to uncertainties in energy losses. Ideally, cross sections selected in the slope-area reach will be uniform and have nearly the same shape and area for a given discharge. In addition, the reach should be long enough and the fall large enough that errors associated with interpretations in the high-water profile are small. In reality, some compromises between logistical considerations and desirable channel properties are typically required. The length of the indirect reach is often limited by the geometry of the channel and the practical difficulties of surveying long reaches of a river channel, and a uniform channel may be difficult or impossible to find.

The Slope-Area Computation Program

The Slope-Area Computation (SAC) Program (Fulford, 1994) has greatly improved the ease of the computation. Input files to SAC supply all required information and the program automates the indirect peak discharge calculation. SAC output includes discharges computed for all cross-section combinations and warnings for reach length, drop, and other

parameters that affect or help evaluate the accuracy of the result.

Sensitivity of Indirect Discharge Computations to Slope

The calculation of accurate discharges using the slope-area method depends on the accuracy of the water-surface elevations, and thus the reach slope, supplied in the input to SAC. Unlike step-backwater calculations, in which the water-surface elevation is specified as a boundary condition at the downstream end (for subcritical flow) and the upstream water surface profile is calculated, the slope-area method for computing discharge imposes a water-surface slope (modified by streamwise changes in velocity head) on the calculation that is used to directly calculate discharge. The sensitivity of the calculated discharge to errors in the reach water-surface drop can be determined by finding the ratio of discharges calculated using the true water-surface slope and the water-surface slope estimated from surveys of reach length and apparent drop in the water surface. The Manning equation is used to compute discharge,

$$Q = \frac{1}{n} AR^{2/3} S^{1/2}, \quad (1)$$

where Q is the discharge, n is the Manning roughness coefficient, A is the cross-section area, R is the hydraulic radius, and S is the water-surface slope. Equation 1 is used with metric units; with Imperial units, the $1/n$ is replaced by $1.49/n$. Representing the surveyed water-surface drop in the reach used to calculate the discharge as the true drop plus an error, the ratio of the true and calculated discharges can be represented by,

$$\frac{Q_c}{Q_t} = \left(1 + \frac{e_c}{d_t} \right)^{1/2}, \quad (2)$$

where Q_c is the discharge calculated with the measured water surface drop, Q_t is the true discharge, e_c is the error in the measured drop in the reach used to calculate Q_c , and d_t is the true drop in the reach. Note that reach length is not represented in equation 2. Small differences in the cross-sectional area and hydraulic radius related to differences in water-surface drops are neglected in equation 2. An example application of equation 2 over a range of errors in reach drop (fig. 1) shows that an error in reach drop of a few tenths of a foot can lead to a calculated discharge that is off by about 25 percent. Equation 1 shows that the discharge is linearly related to cross-sectional area and roughness but is related to the square root of the slope, thus indicating greater sensitivity to channel shape and roughness than slope. Channel shape is well defined by surveys if the channel does not change significantly during a flow event, however, and roughness is generally well defined by published methods for estimating roughness or verified roughness in similar channels.

The Continuous Slope-Area Method

The CSA method expands the slope-area method of computing peak discharge to a complete flow event. Continuously recording pressure transducers (PTs) installed at three or more cross sections provide water-surface slopes and stage during an event that can be used along with cross-section surveys and estimates of channel roughness to compute a continuous-discharge hydrograph. The method, as demonstrated by the applications described in this report, can also reveal complexities during significant flows that are not evident from peak-flow estimates derived from post-flow evidence.

The CSA method has been made feasible by the availability of low-cost recording PTs that provide a continuous record of stage at each cross section. In addition to the applications described in this report, such devices have been used at crest-stage gages to record continuous stage in ephemeral streams (Waltemeyer, 2005). Crest-stage gages were used in this experiment to incorporate standard USGS equipment and methods.

Site Selection

Information about the channel required for the slope-area method is also required for application of the CSA method. A minimum of variability between cross sections and a sufficient drop in the channel are desirable properties. Channel roughness may be estimated using published methods or derived from direct measurements of discharge and water-surface slope. A detailed guide to the slope-area method of discharge is presented by Dalrymple and Benson (1967).

Dalrymple and Benson (1967) indicate that the selection of cross-section locations should be determined by breaks in slope of the water surface profile determined from surveys of debris lines. This method of determining cross-section locations can be difficult to apply where debris lines are poorly defined and is not possible prior to a flow, as would typically be the case for an initial CSA application. Consequently, cross sections for a CSA reach can be located initially, depending on resources available, based on a visual assessment or survey of the reach to identify changes in bed slope or channel width. If sufficient resources are available, a step-backwater model of

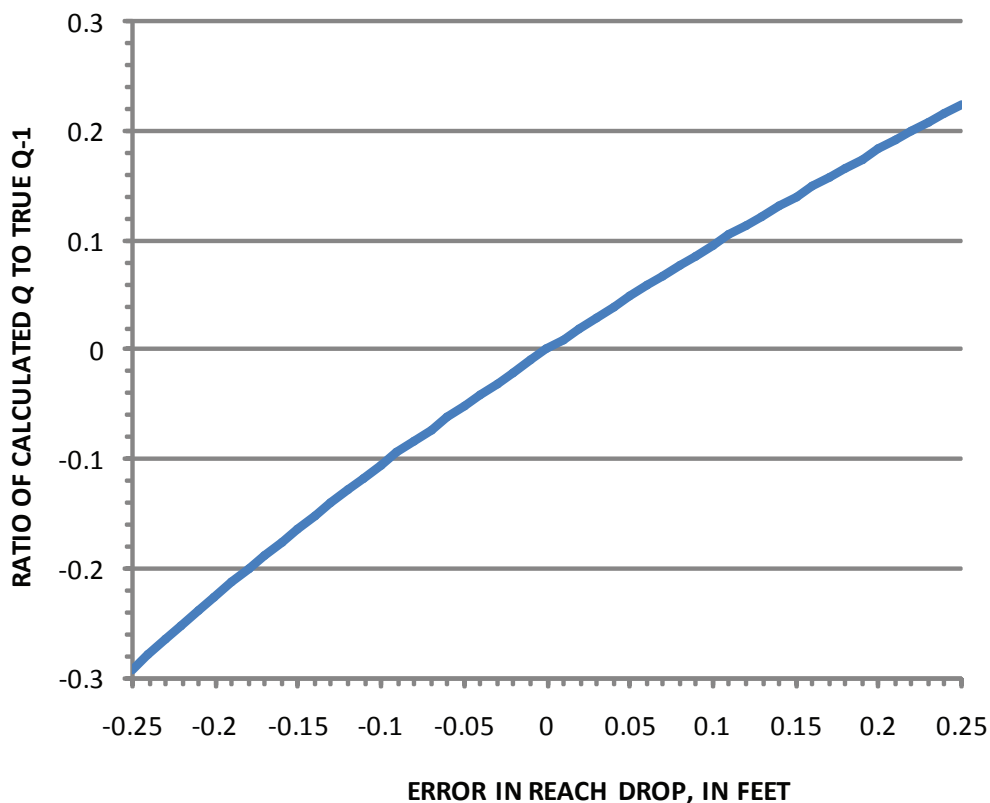


Figure 1. Error in discharge calculated with equation 2, caused by errors in measured reach drop. The sample calculation shown is for a true drop in the reach of 0.5 ft.

4 The Continuous Slope-Area Method for Computing Event Hydrographs

the reach would provide an estimated water surface profile that could be used in accordance with the criteria of Dalrymple and Benson (1967) for cross-section location. After a significant flow has occurred in the reach, cross-section location could be adjusted according to the methods of Dalrymple and Benson (1967) if debris lines are adequate.

Evaluation of Pressure-Transducer Data and Calculated Hydrographs

The calculation of discharge using the slope-area method, on which the CSA method is based, could be accomplished with only two PTs at two cross sections, but at least three cross sections are considered minimum for obtaining reasonably accurate results. The redundancy of multiple cross sections, and possibly more than one PT per cross section, can be an important aid in interpreting stage data and choosing the best sequence of cross sections and stage hydrographs for the discharge calculation and can be critical if instruments malfunction. Including more cross sections in the discharge calculation also increases confidence in the computed discharges.

Irregularities in the calculated-discharge hydrographs can be a result of errors in the PT data, changes in the channel during the flow event, or accurate PT readings that are affected by local conditions such as debris piles, wave action, or isolation from the main flow. The errors in the stage data can come from PT errors, such as time drift and loss of calibration, or CSG errors that can occur from burial or plugging by sediment or from accumulation of local debris. Loss of calibration can be detected by comparing the PT readings with high-water marks on the bank, if clear marks are available, or peak stage was recorded by the CSG. A PT water-surface elevation higher than the high-water marks may indicate a problem with the PT. Changes in the channel during runoff events can include scour, fill, and changes in vegetation along the slope-area reach. Scour may occur at one cross section while fill conditions may affect another cross section during the same flow event. Channel roughness can be modified during floods, if vegetation is bent over or scoured out or if debris collects on trees. All of these conditions need to be identified during the channel survey after the runoff event and considered when evaluating the accuracy of the computed discharge.

Comparison of Pressure-Transducer Peaks to Crest-Stage Gage Peaks

If reliable CSG peak stages or other indicators of maximum stage are available, as in the Babocomari River study reach, they can be compared to the peak stages indicated by the PTs. Differences between the two do not necessarily indicate error in the PT stage, however. The PTs, for example, may miss the peak stage even if they are recording at 5-min intervals.

If the CSG peak stages are recorded in enough cross sections, a slope-area calculation can be made to determine the event-peak discharge. Water-surface elevations from CSGs at

cross-section locations is not as comprehensive as a continuous water surface derived from surveyed debris lines, as is typically used in a conventional slope-area measurement, but CSGs, which are constructed and widely used by the USGS to obtain accurate records of peak stage, may provide more accurate water-surface elevations at cross sections than those inferred from debris lines. The computation can be used to help identify the most favorable cross-section combination for the CSA calculations, and the event peak computed with CSG data can also be compared with the peak discharge calculated with the CSA method to test the accuracy of the CSA method. Because the 5-min recording interval used in the stage recorders may miss the instantaneous peak stage during a flashy event, the CSA peak stage could be less than the event peak. The CSA peak stage can equal the CSG peak stage, but the CSA peak stage should never exceed the CSG peak, unless the CSG is overtopped.

Stage-Discharge Relations

Stage-discharge plots derived from the CSA hydrograph are an effective tool for examining PT performance. The computed discharge is sensitive to the measured fall in the reach. If one or more PTs do not function properly, the computed discharge as a function of stage will be erratic, and a tight relation will not be possible. A tight fit does not assure the accuracy of the stage-discharge relation, but it is an important indicator of the quality of the stage data. If the channel was stable and the instruments performed normally during an event, plots of the calculated discharges against the corresponding stages from each of the pressure transducers should form a tight, consistent plot. If the plot is widely scattered, it likely indicates faulty data or channel instability. A tight plot for medium and high discharge may be accompanied by considerable scatter at low discharges, especially in sand-bedded channels. In this case, the lower discharges may be affected by small-scale channel features that are not significant at higher discharges.

Hysteresis in the Stage-Discharge Relations

The CSA method can be used to make indirect measurements during the rise and fall of the event hydrograph. The data may be used to evaluate differences in hydraulic conditions on the rising and falling limbs of a hydrograph which can cause a loop in the stage-discharge rating curve commonly referred to as hysteresis. Hysteresis in rating curves can be caused by an increase or decrease in the steady-discharge water-surface slope related to the passing of a discharge wave. On the rising limb, the water-surface slope is increased and lowers the stage at a given discharge with respect to the steady-discharge water-surface slope. The opposite occurs on the falling limb of the hydrograph. The magnitude of the hysteresis can be estimated by scaling the terms in the momentum equation using reasonable values for wave speed (which can be estimated from dQ/dA), the rate at which the stage rises or falls, and the steady-discharge water-surface slope (for example, Wiele and Smith, 1996). Changes in roughness or shape

during an event can also cause a loop in the rating curve. In ephemeral channels or channels with low base flow, such as the Babocomari River, vegetation commonly grows within the channel between significant flow events. Channel roughness can be reduced significantly during a large discharge, if vegetation is uprooted and washed downstream or if flexible vegetation, such as grass, is bent over. Conversely, uprooted vegetation can form dams that cause significant backwater effects. Scour or deposition can also contribute to changes in the stage-discharge relation during an event.

Apparent hysteresis can potentially be caused by instrument error or weaknesses in its installation. If the PT position is not firmly fixed, the reference elevation used in the conversion of pressure to stage can change, introducing error into the stage.

Evaluation of Channel Geometry

Changes in channel shape can be determined by comparing cross sections that were surveyed before and after the flow event. After each event, the cross sections should be evaluated to determine if they should be resurveyed. Many small and medium events produce little or no change to the channel and will not require the channel to be resurveyed. High flows, however, can significantly modify the channel, making new surveys necessary. Accuracy of computed peak or continuous discharges can be degraded if significant channel change occurred.

The Effect of Unsteadiness on Discharge Computation Accuracy

The slope-area computation used for indirect discharge measurements and the CSA method is based on an assumption of steady flow. For indirect measurements, this is not an issue because the change in velocity over time is zero at the peak discharge. For computing continuous hydrographs, as in the CSA method, the change in velocity over time is nonzero except at the peak. The significance of neglecting the unsteadiness of the flow can be estimated by considering the relative magnitudes of the terms in the one-dimensional St. Venant equation for momentum,

$$\frac{\partial u}{\partial t} + u \frac{\partial u}{\partial x} + g \left(\frac{\partial e}{\partial x} - S \right) + \frac{u^2}{R_h} = 0, \quad (3)$$

where x is the streamwise dimension, g is gravity, de/dx is the additional water-surface slope due to a varying flow field, S is the steady-flow water-surface slope, u_* is the shear velocity, and R_h is the hydraulic radius. Dividing equation 3 by the driving term, gS , normalizes the equation and reduces the driving term to unity,

$$\frac{1}{gs} \frac{\partial u}{\partial t} + \frac{u}{gs} \frac{\partial u}{\partial x} + \frac{\partial e / \partial x}{s} - 1 + \frac{u^2}{gR_h s} = 0, \quad (4)$$

Taking gravity as a constant, the first term in equation 4 indicates that the significance of the error, induced by using

steady-flow equations to model unsteady flow in the CSA method, is a function of the change of velocity over time and the reach slope. Reaches with steeper slopes are less sensitive to changes in velocity over time than reaches with lower slopes (fig. 2). In the flows on the Babocomari River discussed below, the discharge, and consequently velocity, changes rapidly, but the slope of the reach was about 0.01, which tends to reduce the significance of the unsteadiness on discharge calculations.

Sample calculations with a hypothetical trapezoidal channel (slope = 0.001, bed width = 50 ft, Manning's $n = 0.035$, bank width = two times the depth) illustrate that the velocity and du/dQ tend to change most rapidly with respect to discharge at lower discharges (fig. 3). At the medium and high discharges at which the CSA method is most effective, the relatively muted response of velocity to changes in discharge tends to favor the use of steady-flow equations, but this can be offset by a rapid rise in discharge. During the largest flow on the Babocomari River on July 27, 2006, the normalized unsteady term in equation 4 was not significant (figs. 4, 5), indicating that the accuracy of the computed hydrograph was not significantly affected by the use of steady-flow equations.

Study Site on the Babocomari River

A reach of the Babocomari River was chosen for the initial application and testing of the CSA method (fig. 6). The Babocomari River is a tributary to the San Pedro River in southeastern Arizona, and the study reach and access to it are on Bureau of Land Management land. The elevation of the study reach is 3,980 ft and the drainage area is about 307 mi². The stream is typically perennial with a base flow during the winter of about 1 ft³/s. Peak flows usually occur during the summer months as a result of local convective storms. The streamflow record of the Babocomari River has been used for groundwater studies of the San Pedro basin and the effects of groundwater development on the San Pedro River, a free flowing river that provides vital habitat in an area undergoing rapid population increases and urban development.

There are two permanent streamflow-gaging stations along the Babocomari River. The USGS stream gage Upper Babocomari River near Huachuca City, AZ (identification number 09471380) measures the runoff from the Huachuca and Mustang Mountains (fig. 6). The USGS stream gage Babocomari River near Tombstone, AZ (09471400) was installed for the primary purpose of measuring base flow from a perennial section of the river where groundwater is discharged to the surface (Pool and Coes, 1999). This section of the river is not accessible for medium to high flow measurements.

Starting in the summer of 2002, a CSA reach was selected and monitored on the Babocomari River. The slope-area reach is approximately 0.25 mi downstream from the Babocomari River stream gage (09471400) near Tombstone, AZ. The study site conforms more closely to the criteria established by Dalrymple and Benson (1967) than other reaches in

6 The Continuous Slope-Area Method for Computing Event Hydrographs

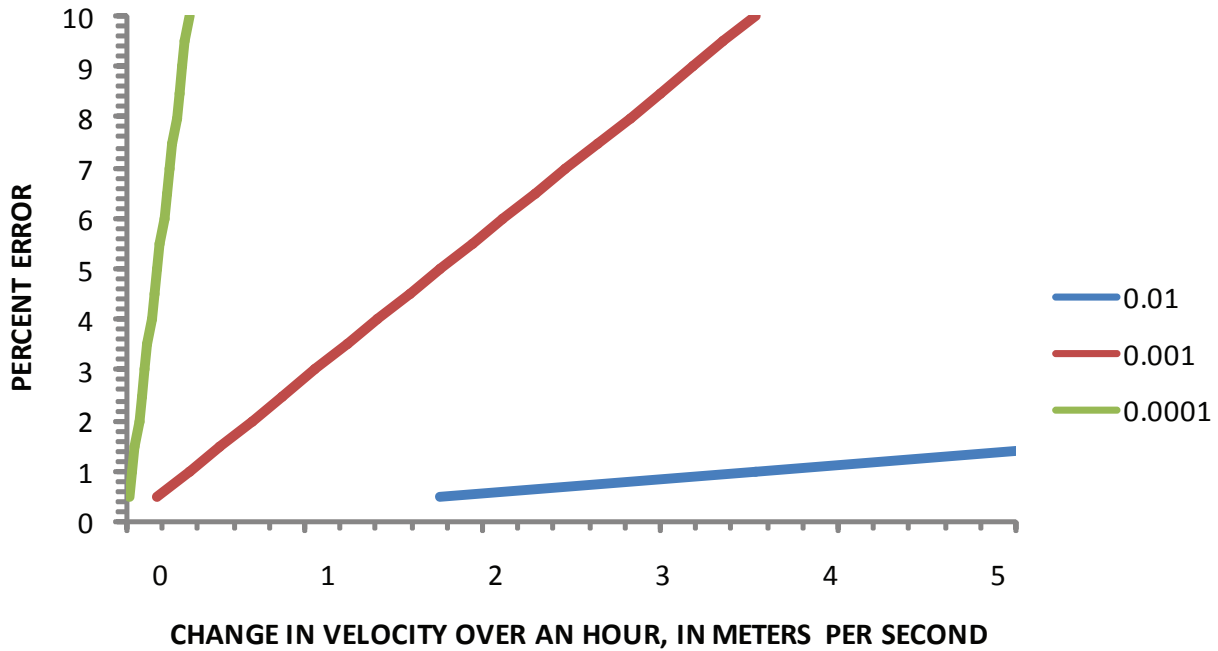


Figure 2. Percent error in the St. Venant momentum equation as a result of neglecting the unsteady term as a function of change in velocity for three reach slopes.

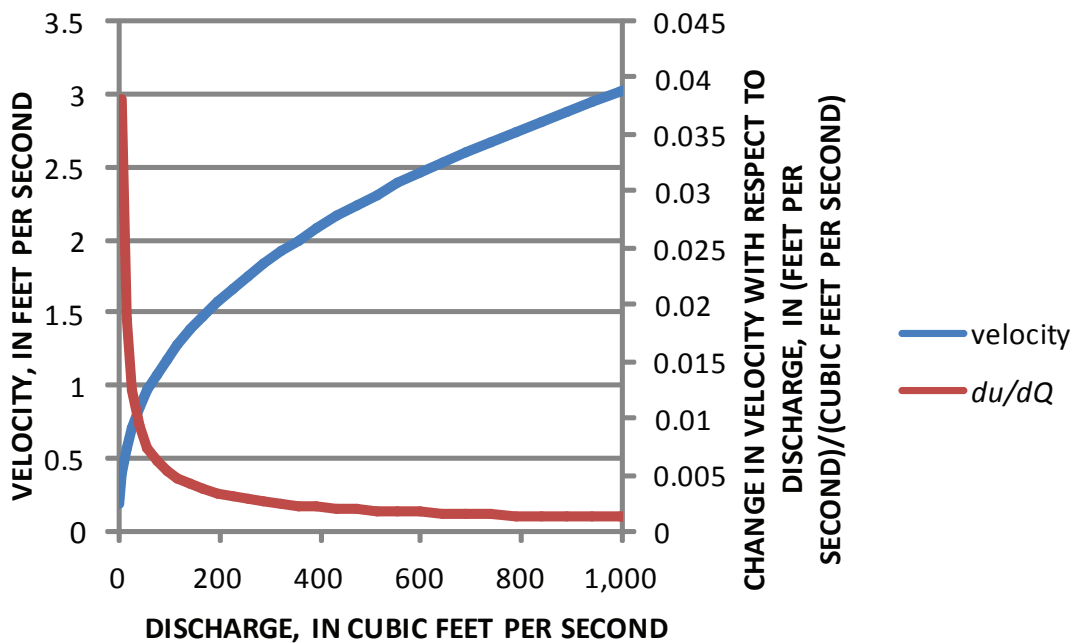


Figure 3. Velocity and du/dQ as function of discharge for a trapezoidal channel with a bed width of 50 ft, slope of 0.001, and a Manning's n of 0.035. The bank width was specified as two times the depth.

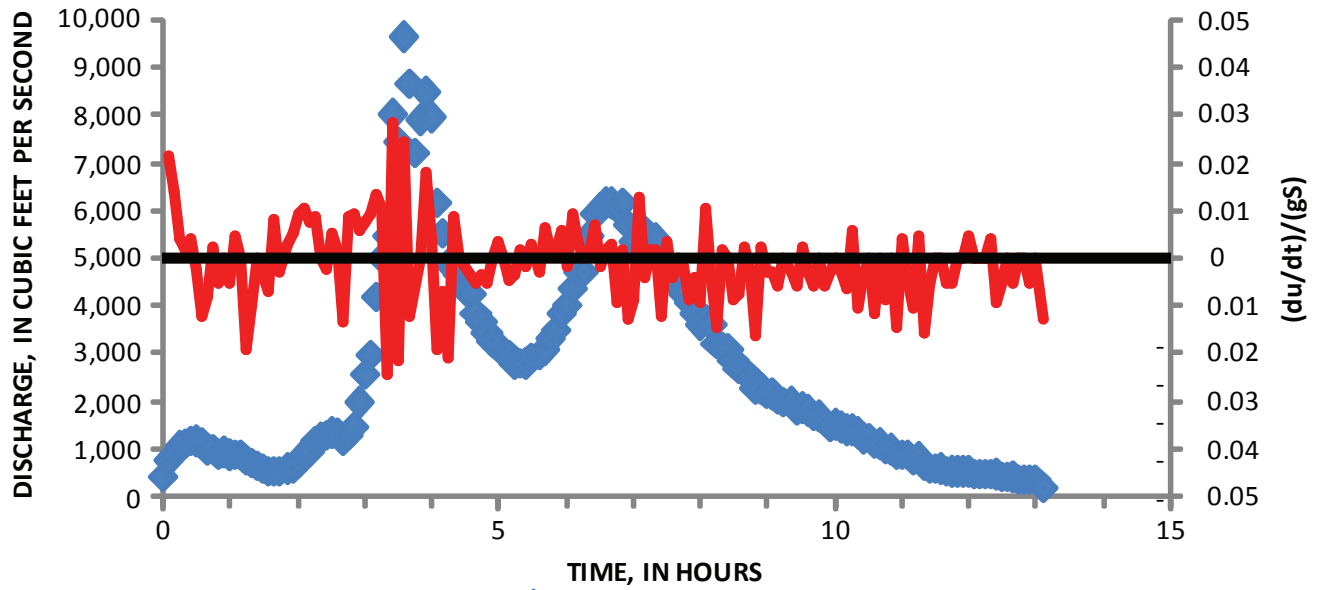


Figure 4. Hydrograph computed with the Continuous Slope-Area method and the normalized unsteady term from the momentum equation $(du/dt)/(gS)$ during the July 27, 2006, event on the Babocomari River.

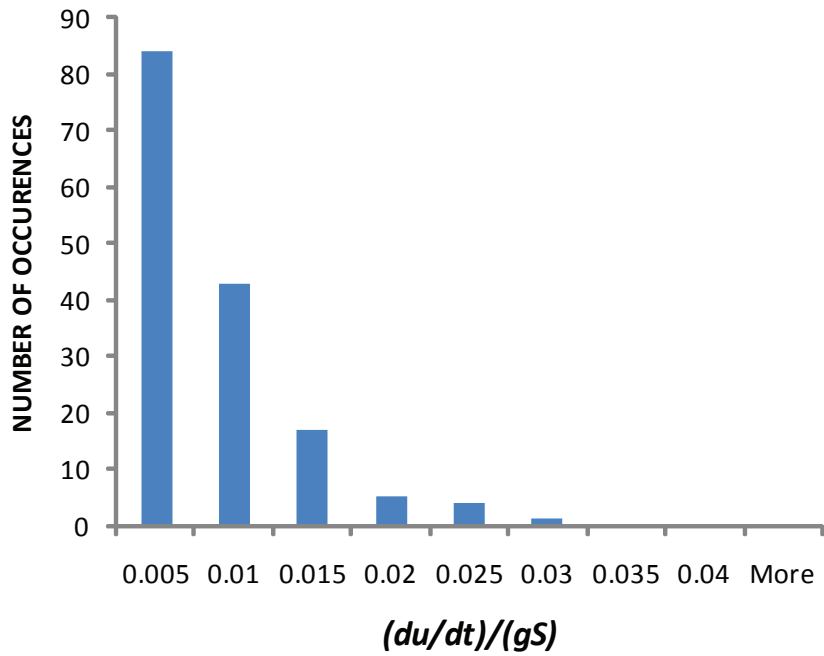


Figure 5. Histogram of the absolute value of the normalized unsteady term in equation 4 for the Babocomari River hydrograph shown in figure 4.

8 The Continuous Slope-Area Method for Computing Event Hydrographs

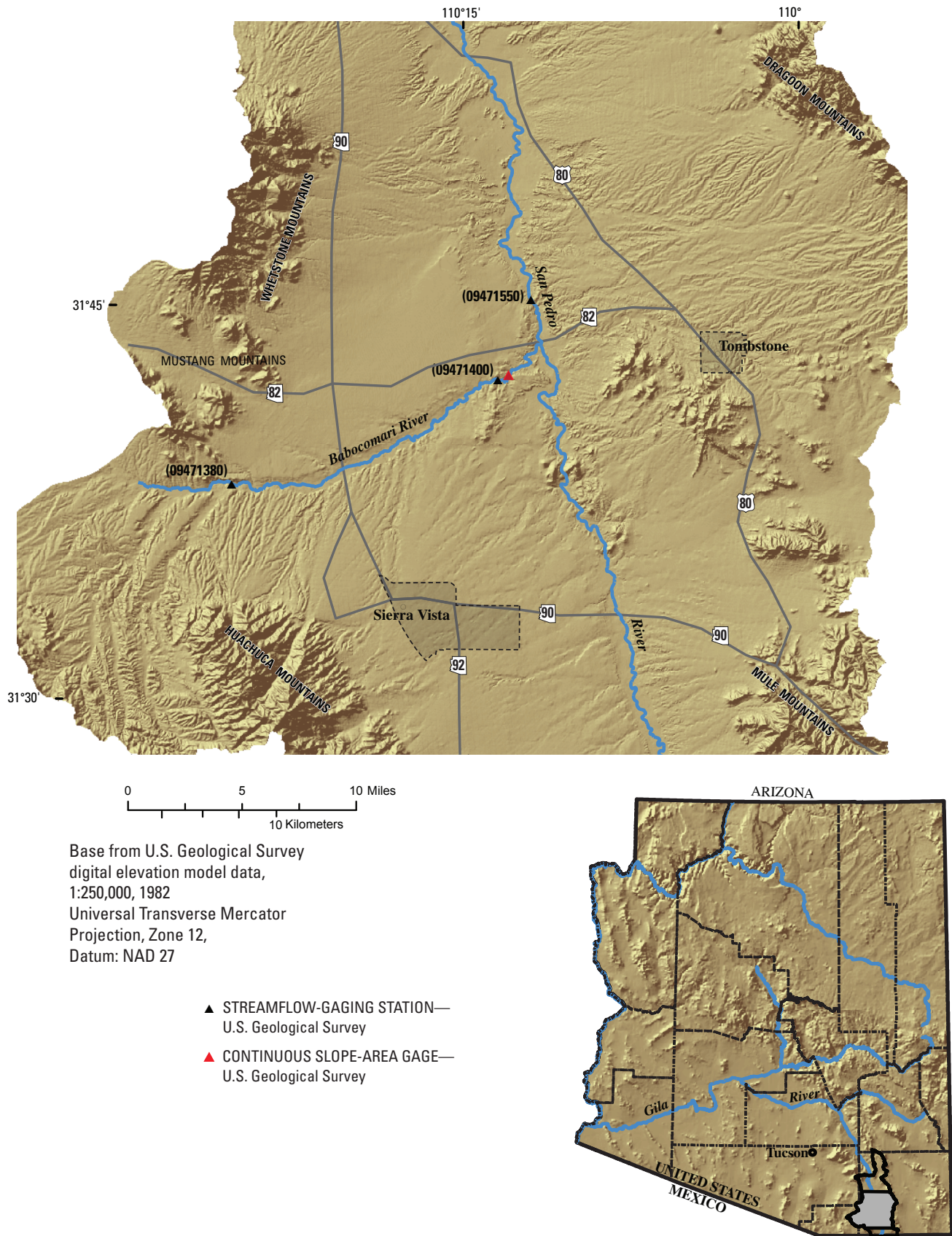


Figure 6. Map showing the study area on the Babocomari River.

the area. At this downstream location, the flow is confined to one main channel. A tributary that flows intermittently enters the river between the gage and the CSA reach.

Description of Channel Conditions along the Slope-Area Reach and Roughness Coefficient Selection

The slope-area reach was selected because it was straight and uniform. The reach is about 300 ft long with about a 2.7-ft fall in water-surface elevation over the range of observed flows. The reach is straight and uniform for about 50 ft above the upstream cross section and 50 ft below the downstream cross section. The total length of the reach was limited by a tributary confluence just upstream of the reach and by an expanding channel downstream of the reach. The cross sections were spaced approximately 100 ft apart.

The grass upstream and downstream of cross section 1 (the upstream extent of the study reach) was dense and consistently about 2 ft tall (fig. 7). The grass throughout the rest of the reach during the study period was sparse on the left bank and dense on the right bank. The density of grass in the reach is related to the density of trees growing in the reach; areas of dense grass are areas of sparse trees. The exposure, absence, or burial of grass in the reach was used to determine if scour or fill occurred during a high-flow event.

The trees in the slope-area reach consist of ash, willow, mesquite, and walnut. The ash and willow are the predominant types of trees growing in the slope-area reach. The younger ash trees (6–14 inches in diameter) line the low-flow

channel and form a ribbon of trees that create barriers on the left bank of the channel and often collect debris (fig. 8).

The willows are not as numerous as the ash trees but tend to be 14 to 20 inches in diameter. There were a few small willows in the low-flow portion of the channel. The mesquite form dense mesquite bosques in the overbank flow areas. A few walnut trees, 10 to 14 inches in diameter, grew on the left bank between cross sections 1 and 2.

A small tributary with a drainage area of less than 0.5 mi² flows into the channel between the gage and the slope-area reach. A PT gage was installed to determine whether inflow from the tributary occurred during main-stem events. The flow from this tributary was not significant during the five events that occurred during the study period and was neglected in the discharge calculations.

The flow through all four cross sections during the study period was contained by steep and well-defined embankments. The vegetation in cross section 1 (X1), the most upstream cross section, consists mostly of grass and small trees (fig. 9). At low flow, the water is contained in a narrow 3-ft-wide channel. The majority of the section is covered with thick grass.

Cross section 2 (X2) is 110 ft downstream of X1 and has a more incised section of flow where the water is ponded at low flow. The vegetation at X2 consists of grass and sapling trees with some mesquite trees higher on the banks (fig. 10).

Cross section 3 (X3), 79 ft downstream from X2, also has an incised section of channel and has vegetation types similar to X2 (fig. 11). A row of ash trees, located on the low-flow section of the left bank starting in X3, extends downstream through cross section 4 (X4).

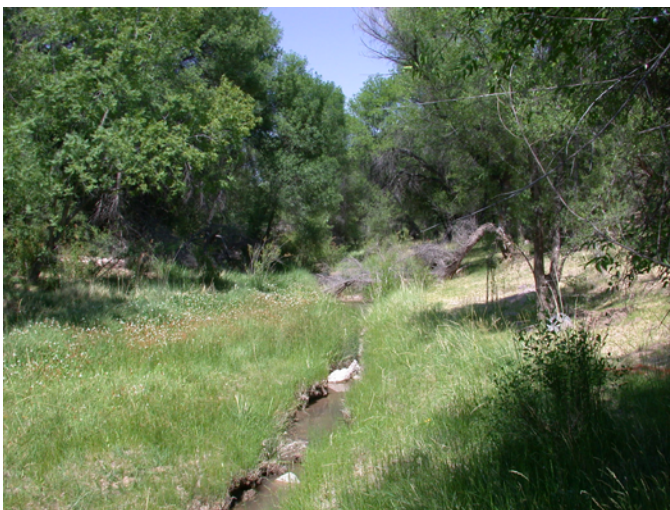


Figure 7. View looking downstream from cross section 1. Note the dense grass where trees are sparse.



Figure 8. View looking upstream from cross section 4. Ash trees grow along the low-flow channel.

10 The Continuous Slope-Area Method for Computing Event Hydrographs

Cross section 4 (X4), 111 ft downstream of X3, does not have an incised channel but has a wider and shallower section of flow. The main section of flow consists of small cobbles and gravels (fig. 12). At low flow, riffles form at this cross section.

A Manning's roughness coefficient was selected based on the type and density of the vegetation in the slope-area reach. Grass is the predominant natural condition that affects the Manning's roughness coefficient for medium and low

flows. For these conditions, a Manning's roughness coefficient of 0.035 was selected for all four cross sections, based on values from reference tables and previous publications (Aldridge and Garrett, 1973; Thomsen and Hjalmarson, 1991; Phillips and Tadayon, 2006). For high flows, the trees along the bank increase the Manning's roughness coefficient to 0.040, which is also based on reference tables and previous publications (Aldridge and Garrett, 1973; Thomsen and Hjalmarson, 1991; Phillips and Tadayon, 2006).



Figure 9. Views from cross section 1 looking upstream (left), downstream (center), and downstream (right).



Figure 10. Views from cross section 2 looking upstream (left), downstream (center), and downstream (right).



Figure 11. Views from cross section 3 looking upstream (left), downstream (center), and downstream (right).

Application of the Continuous Slope-Area Method on the Babocomari River

Installation of Pressure Transducers

The initial installation of PTs for the continuous slope-area application consisted of a modification of the existing crest-stage gage (CSG) design. The CSGs were made of a 4-ft length of 2-in galvanized pipe with a perforated cap on the bottom (fig. 13). The galvanized pipe contains a narrow wooden stick and granulated cork on the bottom cap. During a streamflow event, the cork rises to the peak elevation of streamflow and remains on the wooden stick after the stage recedes, leaving a mark where the crest occurred. PTs were secured to the bottom of the crest-stage gage sticks with hose clamps.

Eight PTs were installed at four cross sections in the overbank area on both sides of the channel (fig. 14). One additional PT gage was installed in a tributary located about 100 ft upstream from the first cross section to document any inflows

between the permanent USGS gage and the CSA reach. Each PT installed in the reach is identified by its location in the reach. For example, PTL2 (pressure transducer 2, left bank) is installed on the left bank and along cross section 2, while PTR2 (pressure transducer 2, right bank) is installed on the right bank. Figure 15 shows the elevations of the CSG pins (used as an elevation reference) on the left and right banks. The streamwise elevation differences between CSG pins on either bank are shown in table 1. On each bank the elevation difference between the farthest upstream and downstream CSG pins is greater than 2 ft. The minimum elevation difference between each CSG pin on the left bank was 0.47 ft, and the minimum on the right bank was 0.07 ft. The CSG pins on the left bank were installed along the overbank area of the channel and are at a higher elevation than the CSG pins on the right bank. The CSG pins on the right bank were installed closer to the active channel. The fall in the reach and between the CSG pins should be uniform, for example the CSG pin in PTR3 should have been installed at an elevation 0.5 ft lower than the pin in PTR2.

The miniTROLL PTs with a sensor range of 0–30 PSI manufactured by In-Situ Inc. were used for this study. The PTs



Figure 12. Views from cross section 4 looking upstream (left), downstream (center), and downstream (right).



Figure 13. Installation of the crest-stage gage (left). The pressure transducer is clamped to the bottom of the crest-stage gage board (center and right).

were programmed to record at 5-min intervals regardless of whether the channel was flowing. In the absence of equipment malfunction, the PT's internal data recorders were capable of measuring and recording pressure at this rate for approximately 6 months. The PTs used for this application measured absolute pressure because they are not vented to the atmosphere. Consequently, in addition to measuring the depth of water above the PT, atmospheric pressure was also measured. To remove the effects of atmospheric pressure, a PT measuring the barometric pressure was placed in the gage house, which is located about 0.25 mile upstream from the slope-area reach.

Collection and Reduction of Pressure-Transducer Data

The stage data were downloaded from the PTs after significant flows. In addition, the cross sections and CSG pin elevations were resurveyed to document any scour or fill in the channel and to ensure the CSG pins had not moved. During each site visit, the CSGs were inspected for high-water marks.

The bottom CSG cap was also removed and inspected to ensure the PT was in connection with the river and not clogged with sediment and debris. After each site visit, fresh cork was added to the CSGs. If high-water marks were present, they were measured and documented. In addition, any other indications of streamflow were noted, such as debris on the base of the CSG and the condition of the vegetation. The PTs were synchronized with atomic clocks to prevent time drift. If time drift was detected, it was documented and the transducer data were corrected. It is imperative that clocks in the PTs are synchronized so that they record water-surface elevations simultaneously during an event.

Each downloaded data set from the PTs was corrected for barometric effects, PT elevation, and CSG pin elevation. The CSG peak was corrected to gage datum by adding the high-water marks from the crest-stage gage to the CSG pin elevation to determine the final peak elevation. After these corrections were applied, both peaks (PT and CSG) were compared for quality control because the PT-recorded peak should not be higher than the CSG high-water mark.

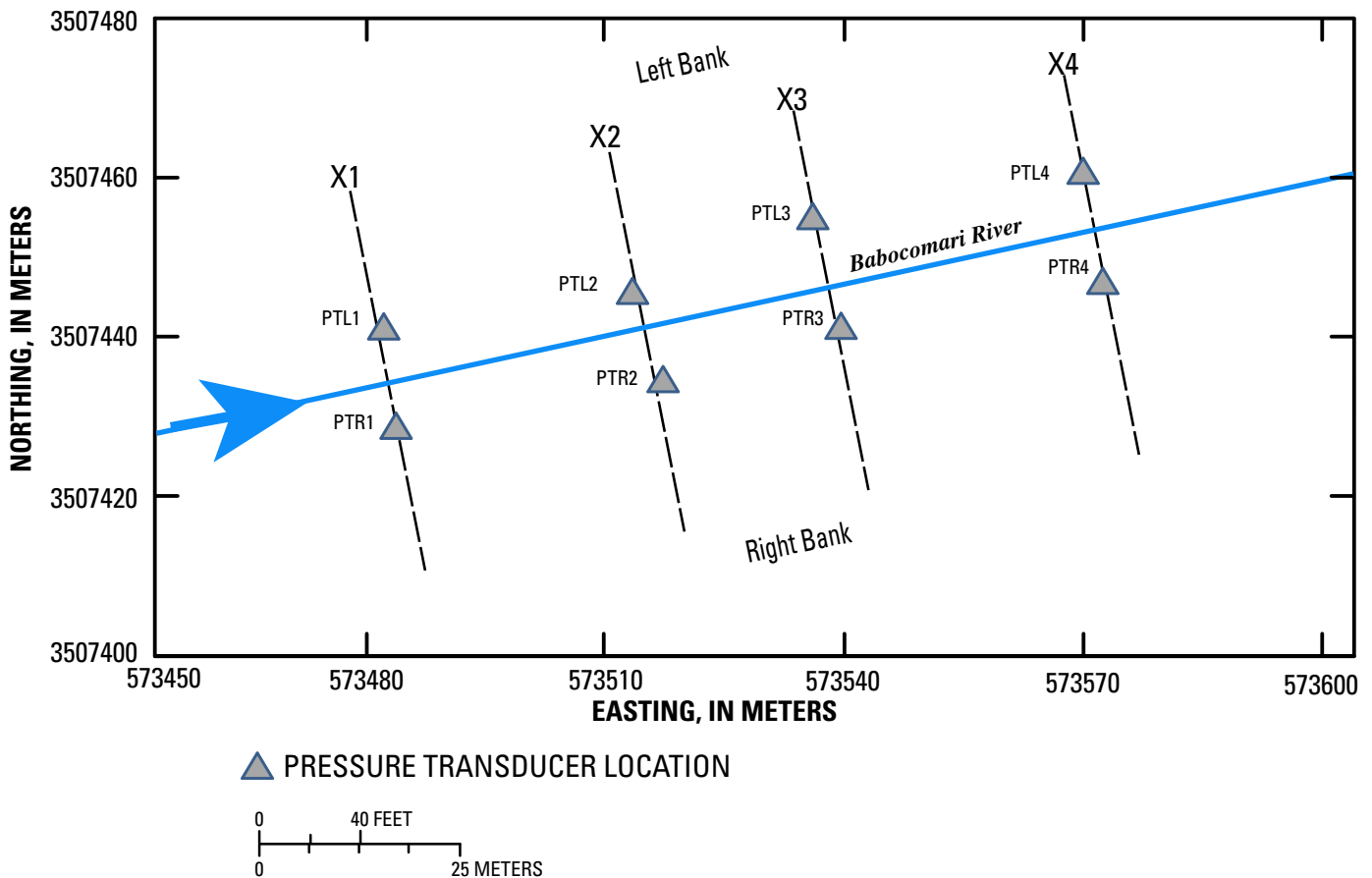


Figure 14. Plan view of the cross sections and eight pressure transducers in the Babocomari River continuous-slope-area reach.

Table 1. Elevation difference between crest-stage and pressure-transducer datums (dry)

Reach	Right-bank elevation difference (ft)	Left-bank elevation difference (ft)
X1-X2	0.52	0.92
X2-X3	0.07	0.69
X3-X4	1.59	0.47
X1-X3	0.59	1.61
X2-X4	1.66	1.16
X1-X4	2.18	2.08

Calculation of Hydrographs Using the Continuous Slope-Area Method

After the necessary corrections were applied to the PT data sets, stage hydrographs were produced from the left- and right-bank pressure-transducer data. The water-surface profiles can be evaluated for comparison with the guidelines recommended by Dalrymple and Benson (1967). The water-surface profiles can show insufficient fall between cross sections, which reduces the accuracy and consistency of the results. A similar practice

is followed with conventional indirect methods, where high-water marks and cross sections can be removed from the final calculation to improve the quality of discharge computations. Following the initial evaluation of the stage data, discharges are computed with the SAC program.

Batch-Processing Discharge Computations

The calculation of the continuous discharge is accomplished by applying the SAC program to each step in the

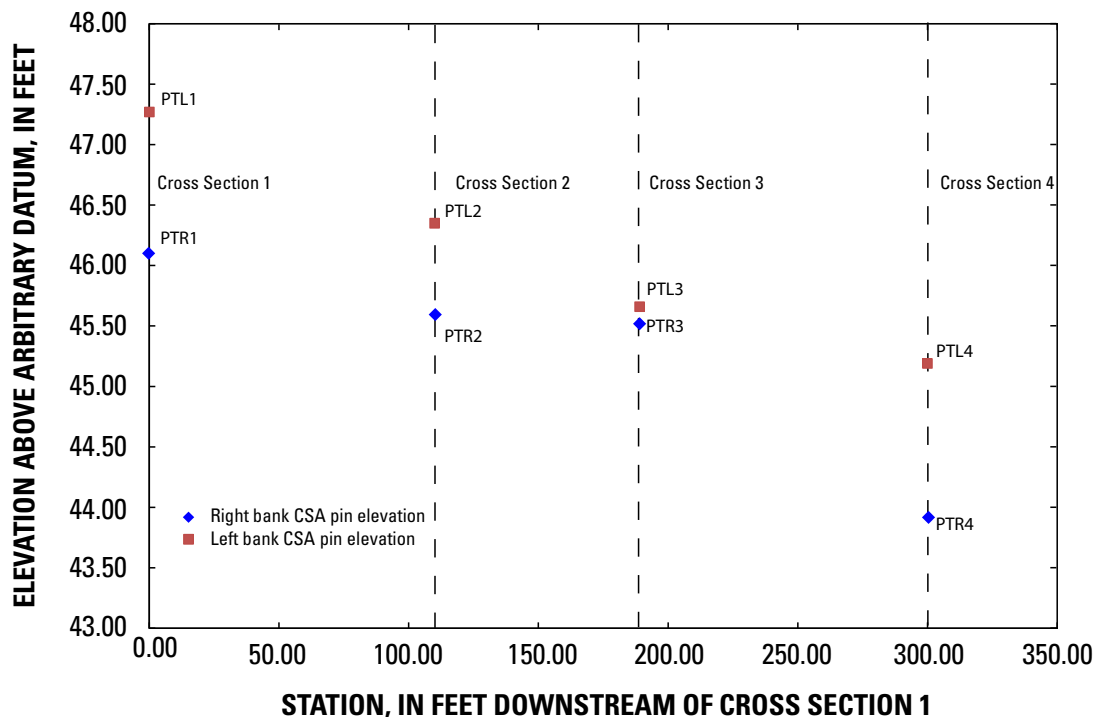


Figure 15. Pressure-transducer-pin elevations (dry with no flow).

stage-time series. This procedure was automated with a utility program (CSA2SAC) developed for this project that reads in the channel parameters used in the SAC program and the stage data, generates the SAC input files for each time step, runs the SAC program for each time step, reads the SAC output files, and finally generates a separate file containing the computed hydrograph.

Development of Stage-Discharge Relations

A stage-discharge relation can be created from the stage data collected by any of the PTs and the discharge data computed by the SAC program. The development of stage-discharge relations is generally best achieved by using the discharges computed using more than two cross sections. The multi-section reach computation averages reach conditions, producing a more consistent discharge.

Major Flows on the Babocomari River 2002–2006

During the five-year study period, Arizona experienced one of the driest periods ever recorded, so medium- and high-flow events were less frequent than normal (Phillips and Thomas, 2005). Five events that inundated the CSG and PT gages occurred during the study period and, as a result, were

sufficiently large for the application of the CSA method (table 2; fig. 16). The events between 2002 and 2005 were moderate flows of similar magnitude. The width of flow for these events was about 80 ft. During flow in 2006, which was the largest during the study, the width of flow exceeded 150 ft and depths were over 12 ft. The following sections describe one of the four moderate events (October, 2003) and the high flow in 2006 to illustrate the CSA application under field conditions. Stage data, computed discharges, and channel shape and roughness for all five events are recorded in appendices 1 and 2.

Flow of October 9, 2003

A moderate event occurred on October 9, 2003, that was caused by a late-season monsoon. The streamflow event lasted about 1 hr, and the water-surface elevations were high enough to submerge all eight PTs for 20 min. The recorded stage hydrographs from each of the PTs are shown in figure 17.

Channel Geometry

The channel geometry surveyed before and after the October 9, 2003, flow event indicates little channel change during the event (figs. 18–21).

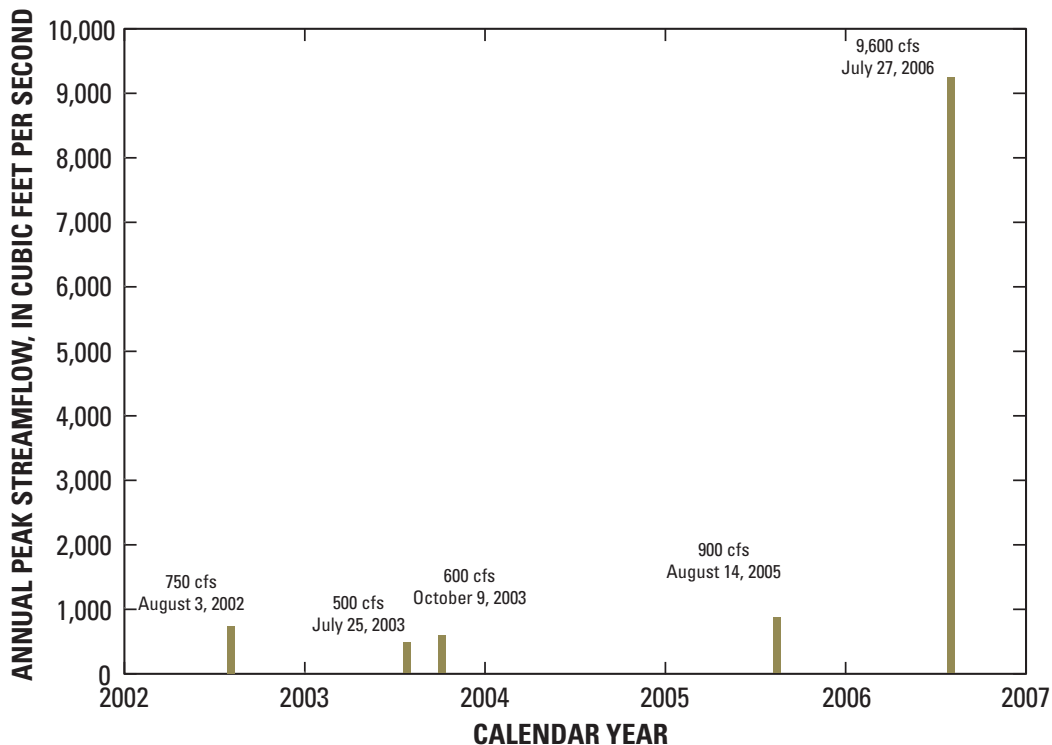


Figure 16. Peak streamflows recorded on the Babocomari River during the study period, 2002–2006.

Table 2. Peak stages recorded by the crest-stage gages and by the pressure transducers during the October 9, 2003, event.

Pressure transducer (PT) (R, right; L, left)	Crest-stage gage height (feet)	Peak (ft) and time recorded by the PT
PTR1	47.33	47.30 at 19:55
PTL1	47.54	47.49 at 19:55
PTR2	47.17	47.00 at 19:55
PTL2	47.22	47.10 at 19:50
PTR3	46.53	46.38 at 19:50
PTL3	46.71	46.63 at 19:55
PTR4	46.33	46.34 at 19:55

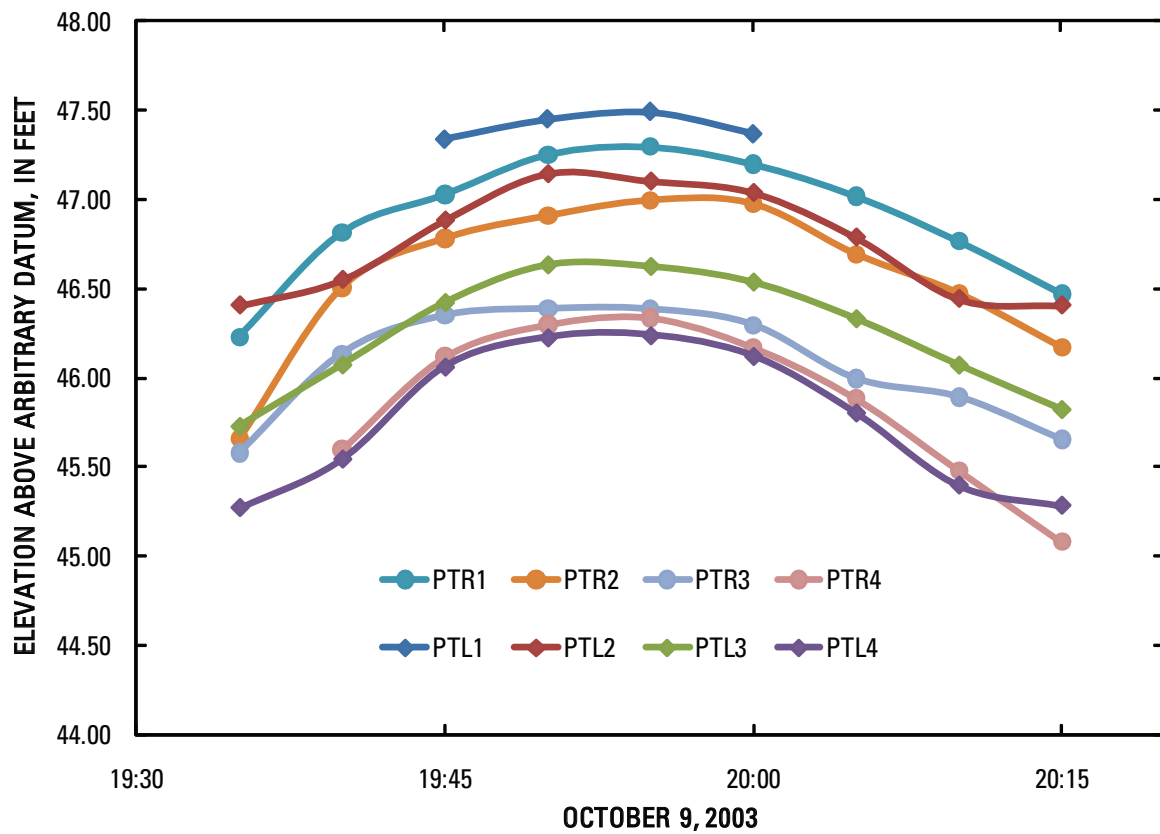


Figure 17. Stage hydrographs from the October 9, 2003, flow event on the Babocomari River.

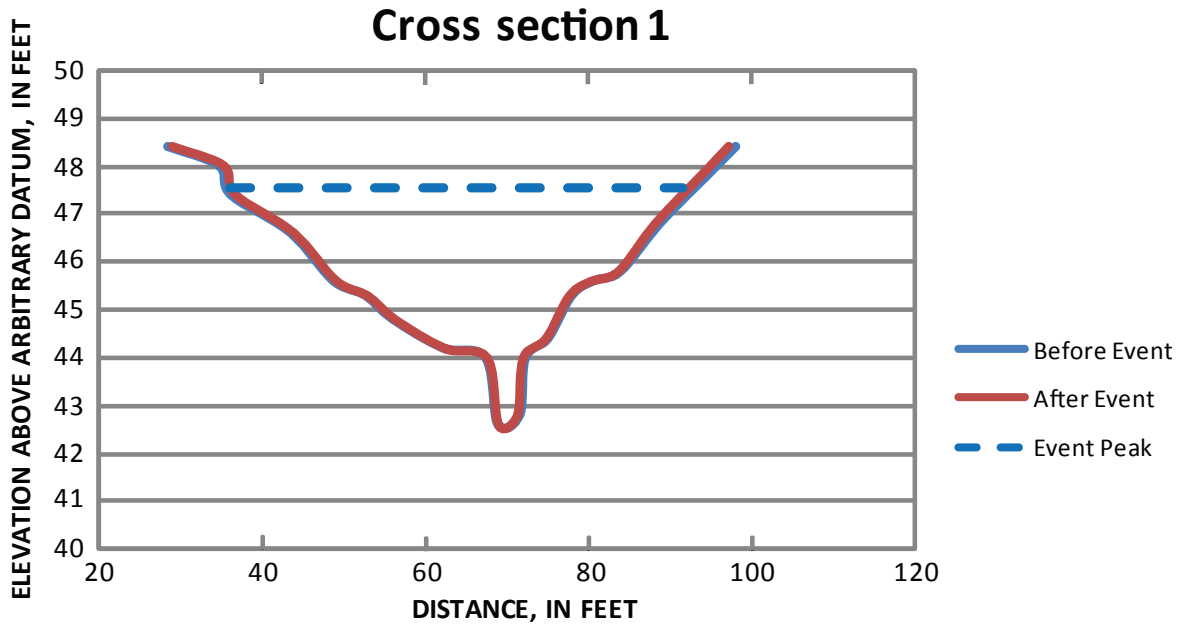


Figure 18. Channel surveys in cross section 1 before and after the October 9, 2003, event. The blue dashed line shows the water-surface elevation at the peak discharge.

Evaluation of the High-Water Marks

Crest-stage gage heights representing the crest of the peak were present on all eight of the crest-stage gages following the flow event. The crest-stage gage heights and the

PT-recorded peak values and times associated are shown in table 2. On the left bank, the crest-stage gage heights were higher than the recorded PT peak values; on the right bank, the recorded PT peak values were within 0.01 ft or less than the crest-stage gage heights, with the exception of PTR4 that

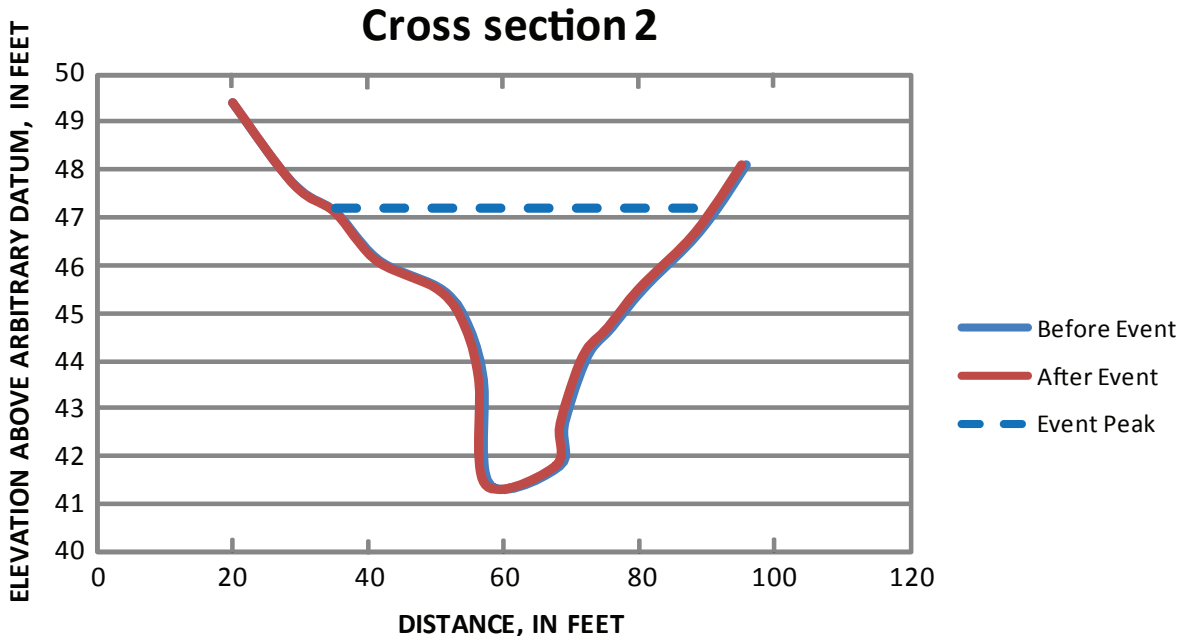


Figure 19. Channel surveys in cross section 2 before and after the October 9, 2003, event. The blue dashed line shows the water-surface elevation at the peak discharge.

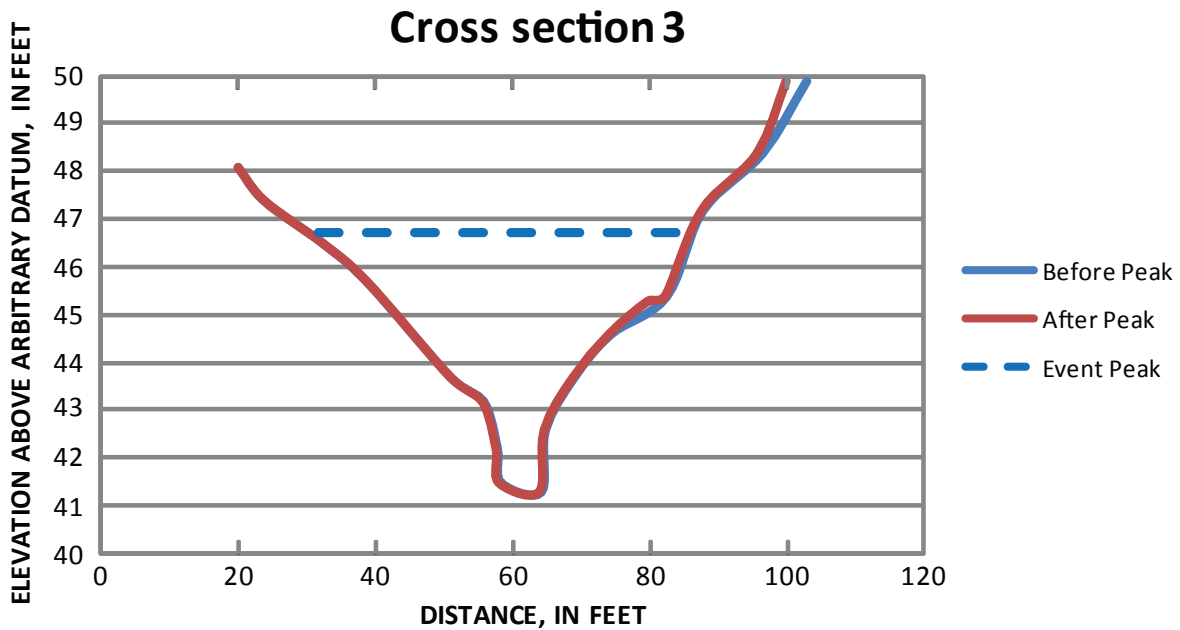


Figure 20. Channel surveys in cross section 3 before and after the October 9, 2003, event. The blue dashed line shows the water-surface elevation at the peak discharge.

recorded the same water-surface elevation as PTR3. Six of the eight PTs recorded the peak water surface at 19:55, while two PTs recorded the peak at 19:50. The difference between these peak times could be attributed to splashing or wave action.

Conventional Slope-Area Computation and Analysis

A slope-area calculation using the corrected CSG elevations at four cross sections was performed. A Manning's n value of 0.035 was judged appropriate for each of these four

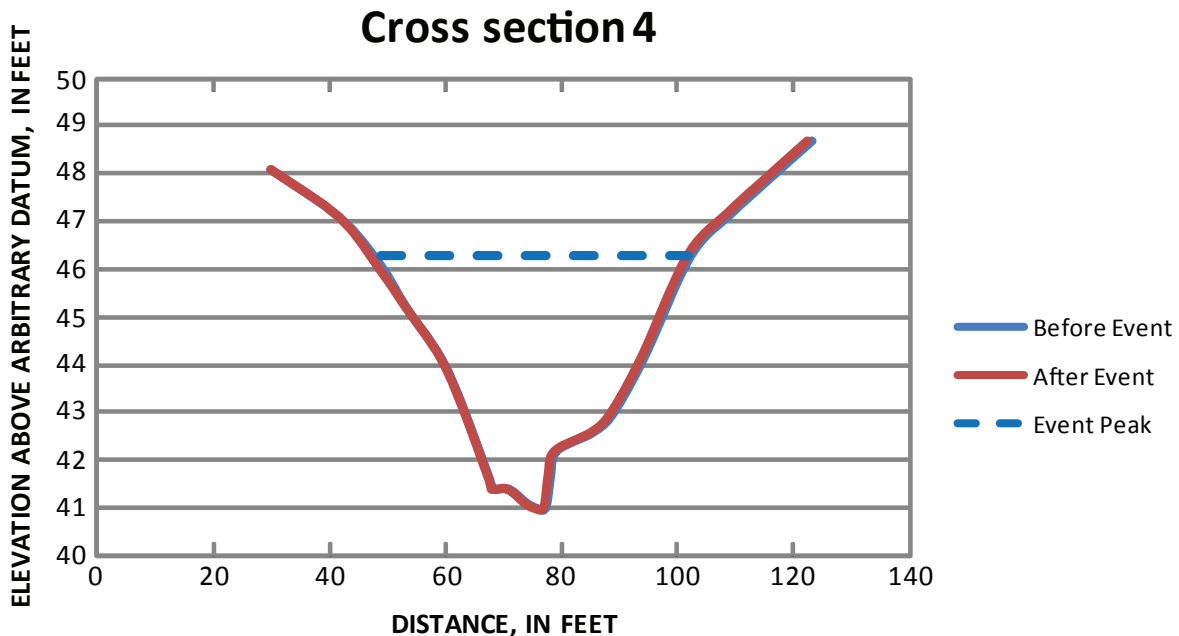


Figure 21. Channel surveys in cross section 4 before and after the October 9, 2003, event. The blue dashed line shows the water-surface elevation at the peak discharge.

Table 3. Peak discharge for cross sections 1–4, based on average of left and right stage data from the pressure transducers and crest-stage gage from the October 9, 2003, event.

Peak discharge computed from the crest-stage gage heights (ft ³ /s)	Peak discharge computed from the PT recorded elevations (ft ³ /s)
626	591

cross sections based on channels with similar conditions in southeastern Arizona (Aldridge and Garrett, 1973; Phillips and Tadayon, 2006). The computed discharge, using the average of the left and right crest-stage gage heights, was 626 ft³/s (table 3).

Evaluation of the Pressure-Transducer Data

The left and right averaged PT-stage values used for the CSA computation are shown in figure 22. The average of the left- and right-bank water surfaces results in a hydrograph that represents the water surfaces during the flow event. The four hydrographs contain water-surface elevations recorded nine times during the 40-minute event.

Continuous Slope-Area Discharge Computations and Analysis

The discharge values computed from the average peak left and right CSG heights and the recorded PT-gage heights are shown in table 3. The CSA-computed discharge values ranged from 340 to 591 ft³/s during the streamflow event. The computed peak discharge using the CSG heights (626 ft³/s) was 35 ft³/s greater than the computed peak discharge from the PTs (fig. 23).

Rating Development

A stage-discharge relation was developed showing the relation between the discharge computed with the CSA

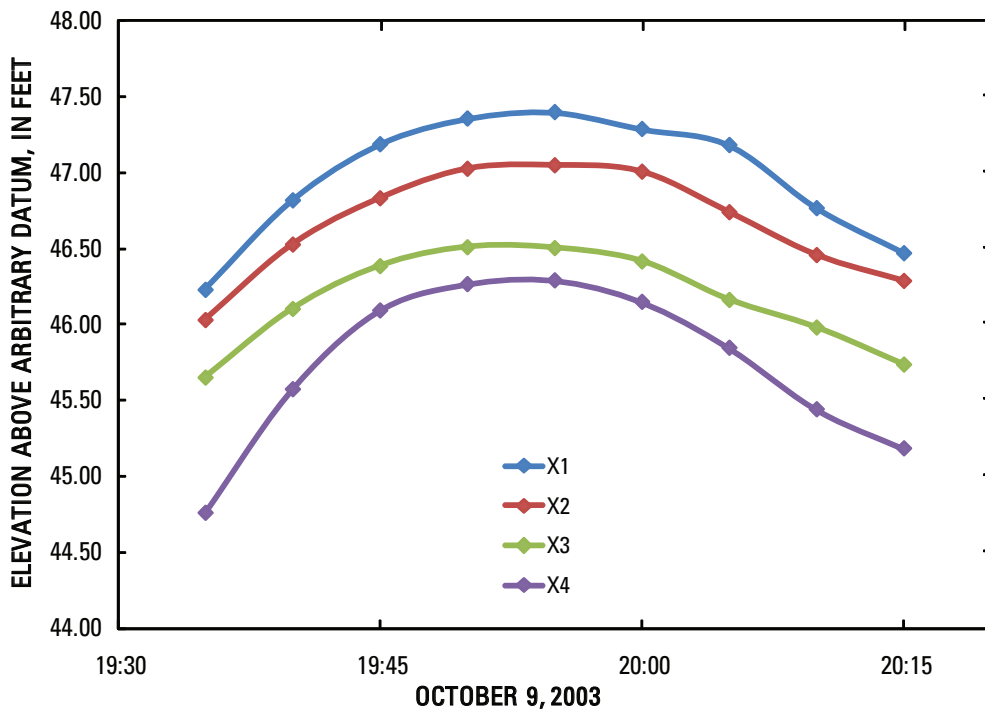


Figure 22. Average left- and right-bank pressure-transducer-stage hydrographs during the October 9, 2003, event.

method and stage from PTR1 (fig. 24). Stage values from PTR1 were selected over the stage values from the other PTs, because PTR1 stage values produced the closest fit in the stage-discharge relation. The single discharge value calculated from the CSG heights was also included in the plot and is consistent with the CSA results.

Summary of the October 2003 Event

The third flow event of the study period occurred on October 9, 2003, and all eight of the PTs were submerged and recorded stage during part of the 1-hr event. Crest-stage gage heights were also obtained from eight of the CSGs. Slope-area calculations were performed to determine the peak streamflow using both data from the PTs and the CSG heights. The computed peak discharge value from the CSG heights was about 6 percent higher than the peak discharge value calculated from the peak PT values.

The Flow Event of July 27, 2006

The July 27, 2006, event produced the peak of record, 9,600 ft³/s, which had an annual exceedance probability of 4 percent. This peak was nearly 10 times greater than any of the previous peaks during the study. Six out of the eight PTs

collected data for this event (fig. 25); two PTs (PTR2, PTL4) did not work due to lost battery power. All four cross sections were used in the analysis.

Five of the six PTs that worked for this flow event were rotated about their base shortly after the peak. The pipes supporting PTR1, PTL2, PTR3, PTL3, and PTR4 were all rotated about 45° (fig. 26) in the downstream direction; only PTL1 remained upright. The five PTs continued to record throughout the event, but only data obtained prior to their displacement were used in the analysis. A sudden shift of about 0.3 ft in stage at each PT indicated the time at which the PTs were displaced.

Changes in Channel Shape

The only measureable change to the reach during the study period was caused by the July 27, 2006, flood. Two trees were uprooted and deposited near the PTs in X1 and X2 but appeared to have minimal effect on the cross-sectional areas of X1 and X2. Vegetation debris accumulated near X3, and sand and gravel were deposited near X4. The changes are generally minor, and their effects on channel hydraulics over the course of the event were neglected in the discharge calculations (fig. 27). The channel changes, however small, introduce additional uncertainty in the computed hydrograph and illustrate another

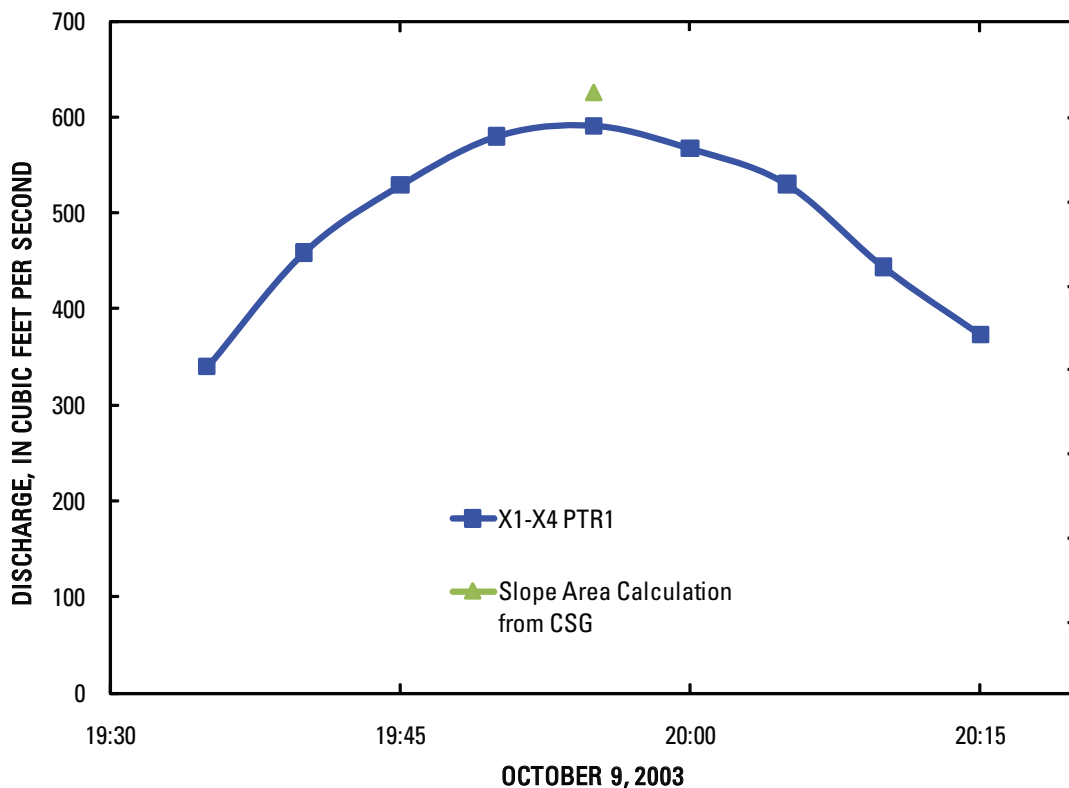


Figure 23. Discharge values computed with the average pressure-transducer and crest-stage gage data for the October 9, 2003, event.

source of potential error that is present in any kind of hydraulic reconstruction of a significant flow, whether it is step-backwater modeling, multi-dimensional hydraulic modeling, peak-flow indirect measurements, standard stream gaging, or CSA applications. The precise timing of the changes to channel shape is unknown but likely occurred near the peak discharge. Gravel deposited near the right bank in X1 caused a 2 percent decrease in the peak-flow cross-sectional area (fig. 28). Scour in the thalweg and the left side of the channel caused an 8 percent increase in cross-sectional area in X2 (fig. 29). In X3, a 0.5 percent increase occurred as a result of scour in the center of the channel (fig. 30). There was a 4 percent decrease in cross-sectional area in X4, caused by deposition of sand and gravel in the center of the channel (fig. 31).

Evaluation of the High-Water Marks

High-water marks from the CSGs were not present, because the CSGs were overtopped. Instead, surveyed high-water marks were used in the slope-area computation, although high-water marks were not preserved on the large rocks that dominate the left bank at X1 and X2. The large rocks were present on the left bank 50 ft upstream of X1 and

extended continuously downstream through X2. The surveyed high-water marks combined with the peak stage values from the PTRs are shown in table 4. The peak recorded from PTR3 of 56.95 ft was greater than the high-water mark of 55.79 ft surveyed in X3 on the left bank. This may have been caused by debris that accumulated in the center of the channel, which caused an elevated water surface next to PTR3, but did not extend far enough along the bank to elevate the left-bank high-water mark or to affect PTR2.

Slope-Area Computation and Analysis of High-Water Marks

A slope-area calculation of the peak discharge using the surveyed high-water marks at the four cross sections was performed. A Manning’s *n* of 0.040 was selected, which is greater than the value of 0.035 used in previous flow events. The *n* value was increased to account for debris that was collected on trees and bushes in the slope-area reach, and the fallen trees that collected deposits of sand and gravel.

The fall between cross sections X3-X4 on the left bank was 0.60 ft, and a discharge of 12,044 ft³/s was computed (table 5). On the right bank, the subreach X1-X2 had an inverse slope

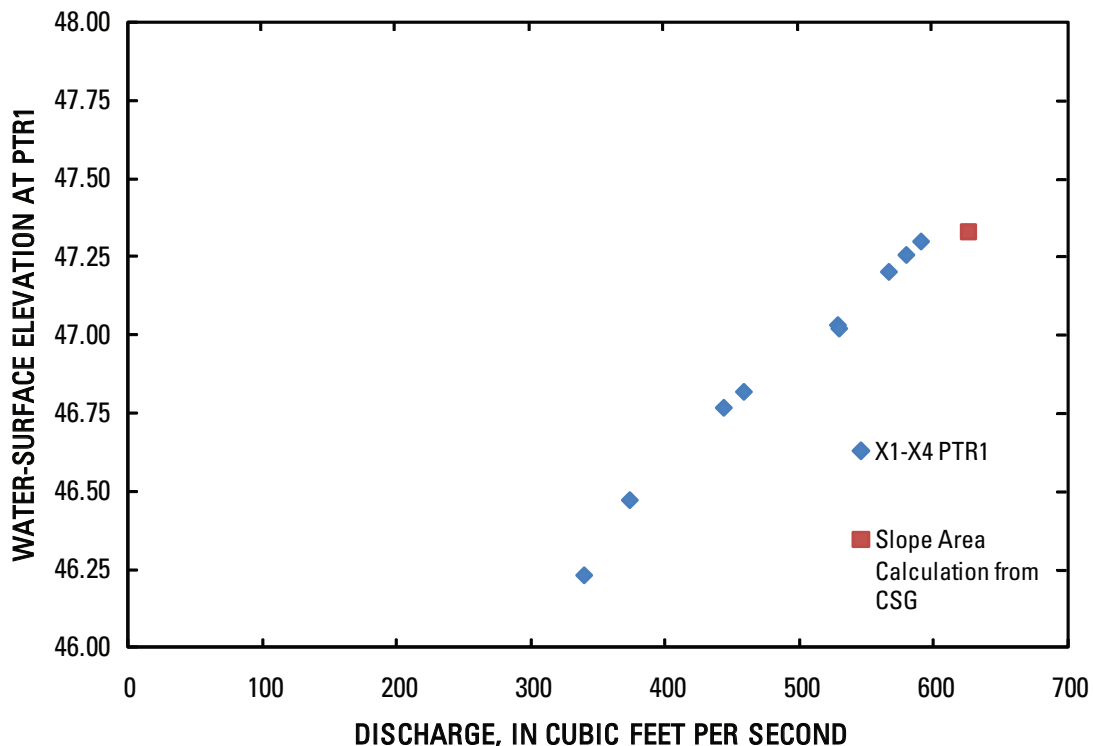


Figure 24. Stage-discharge relation determined with discharges computed from the averaged pressure-transducer data and crest-stage gage data for the October 9, 2003, event.

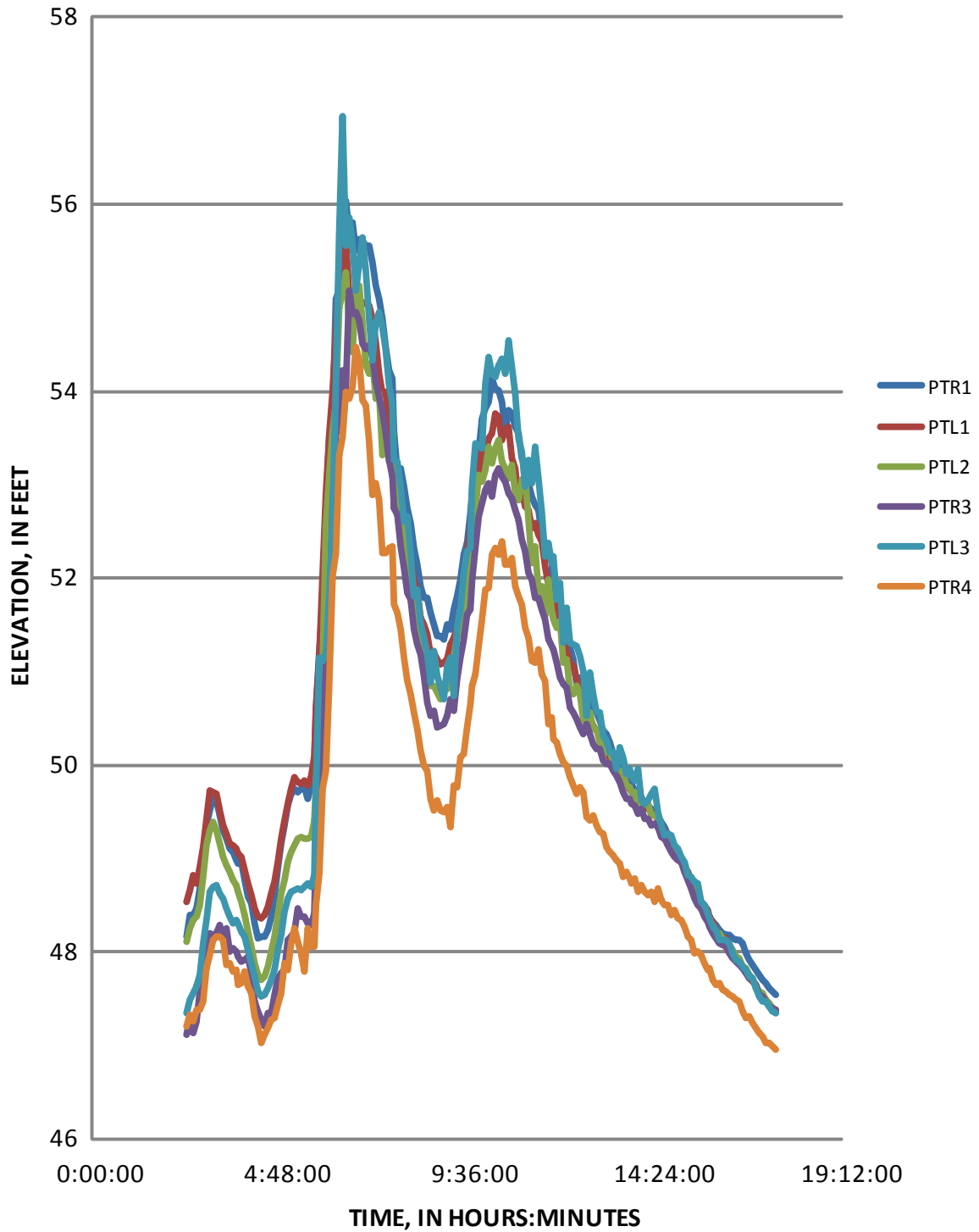


Figure 25. July 27, 2006, stage hydrographs for six pressure transducers. Right-bank pressure transducers are indicated by R in the legend label; left-bank pressure transducers are indicated by L in the legend label; the number in the legend label corresponds to the cross-section number.



Figure 26. Right-bank pressure transducer in cross section 1 (PTR1) after the July 27, 2006, flow event.



Figure 27. View looking upstream from cross section 3 on the right bank after the July 27, 2006, event. The floodway is mostly clear of obstacles.

and, therefore, that combination of cross sections could not be used to compute discharge. The discharges computed with right-bank elevations ranged from 7,818 ft³/s to 12,409 ft³/s (table 6). The most consistent results came from the multiple cross-section reaches X1-X3, X2-X4, and X1-X4.

Slope-Area Computation of Peak Discharge using PT Data and Analysis of PT Data

The peak discharge was computed using the slope-area method and peak PT elevations from the left (table 7) and right (table 8) banks. The results of the left-bank slope-area

computation of discharge showed that only one subreach, X1-X2, could be used in the analysis as a result of the debris pile downstream. The fall between X1-X2 was 0.33 ft and the computed discharge was 8,466 ft³/s.

The peak stage values from the right bank produced a small range in computed discharge of 9,138 ft³/s to 10,589 ft³/s (table 8). The discharge computed using stage values from the right bank (X1-X4) of 9,621 ft³/s was considered the discharge most likely to be accurate from the slope-area computations, because it uses the longest reach and incorporates more channel data than the other cross-section combinations.

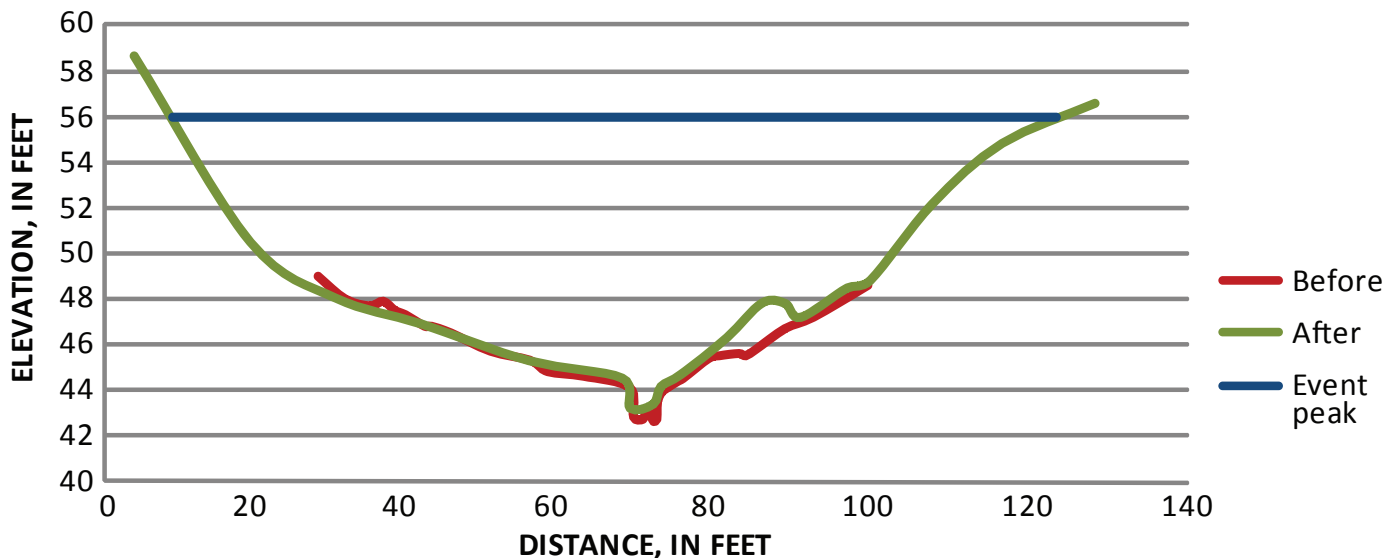


Figure 28. Channel surveys in cross section 1 before and after the July 27, 2006, event. The blue line shows the water-surface elevation at the peak discharge. At the peak discharge, the difference in cross-section areas is 2 percent.

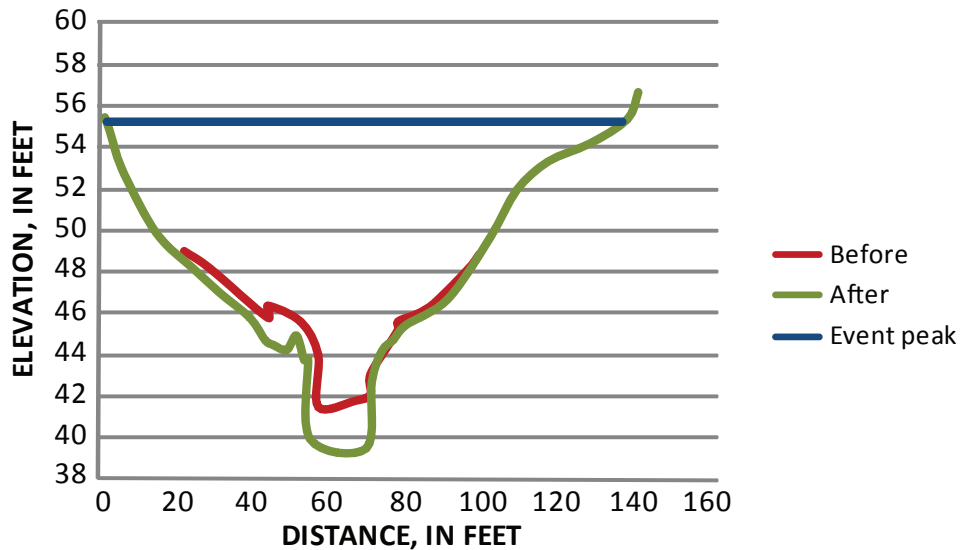


Figure 29. Channel surveys in cross section 2 before and after the July 27, 2006, event. The blue line shows the water-surface elevation at the peak discharge. At the peak discharge, the difference in cross-section areas is 8 percent.

Evaluation of the Pressure-Transducer Data

Data from the six working PTs were evaluated to determine the optimum combination for discharge computations. PTL3 was not used because of the elevated stage effects from the accumulated debris (fig. 32). The remaining five PTs were PTR1, PTR3, and PTR4 from the right bank and PTL1 and PTL2 from the left bank. Because the right bank high-water

marks and pressure-transducer peaks produced a narrower range of discharges in computing the slope-area discharges, the right bank PTs were used along with PTL2, which was the only sensor available for X2, for the final discharge computation. PTL1 was not used in the computation of discharge, but, because it was the only PT not displaced during the event, it was used for the stage record in developing the event-rating curve and the event-discharge hydrograph.

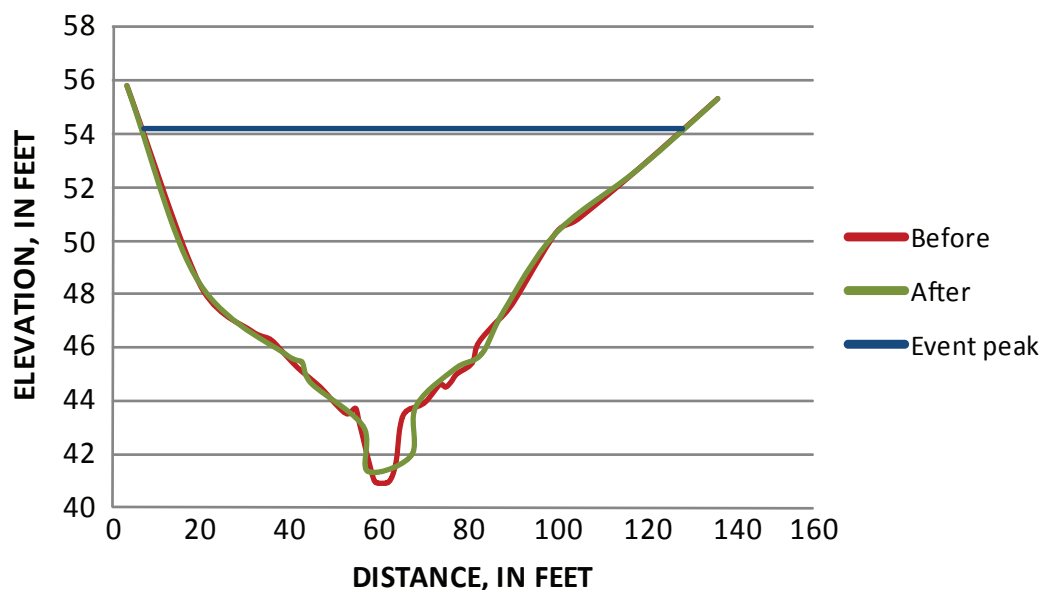


Figure 30. Channel surveys in cross section 3 before and after the July 27, 2006, event. The blue line shows the water-surface elevation at the peak discharge. At the peak discharge, the difference in cross-section areas is 0.5 percent.

Stage hydrographs from PTR1, PTL2, PTR3, and PTR4 (fig. 33) were selected to compute discharge. The CSGs attached to these PTs were rotated to about a 45° angle from vertical just after the flow peak and, consequently, discharge values were not computed after the peak. The event-rating curve was developed from discharge values computed using stage values that were recorded prior to the PTs being displaced.

Development of Stage-Discharge Relation

The stage-discharge relation was developed from stage values from PTL1 and discharge values computed with stage values recorded before the PTs were knocked over (fig. 34). A log function fit to the stage-discharge points has a R^2 of 0.9957, indicating that the stage-discharge relation fits the data closely with little scatter.

Transfer of the CSA Stage-Discharge Relation to the Babocomari River near Tombstone Streamflow-Gaging Station

The July 27, 2006, flood removed most of the large trees that were growing in the channel reach above and below the Babocomari River near Tombstone

streamflow-gaging station, about 0.25 mi above the CSA site (fig. 8). The large trees in the channel bottom were the controls for the medium to high flows near the gage (fig. 35). This is a common condition at many USGS streamgages in Arizona. Periods of low or no flow allow dense vegetation growth in the channel that can significantly modify the channel hydraulic properties.

During the July flood, nearly all of the vegetation in the channel near the gage was removed near the flood peak and during the recession. In contrast, the same flood only caused minor changes in the downstream CSA reach. The stage-discharge relation for the Babocomari River near Tombstone gage depends on the condition of vegetation in the channel and was altered by the removal of vegetation during the July 27, 2006, flood. Consequently, a new stage-discharge relation was developed for the gage. The stage-discharge relation will return to its pre-flood form as the vegetations grow back in the channel.

The stage hydrograph from the Babocomari River near Tombstone gage was compared with the stage hydrograph from PTL1 (fig. 36). The two hydrographs matched until just after the peak, when the gage hydrograph diverges from the PTL1 hydrograph, most likely as a result of the scouring of vegetation from the gage reach. On the recession, the gage hydrograph drops more than the PTL1 hydrograph by as much as 3 ft.

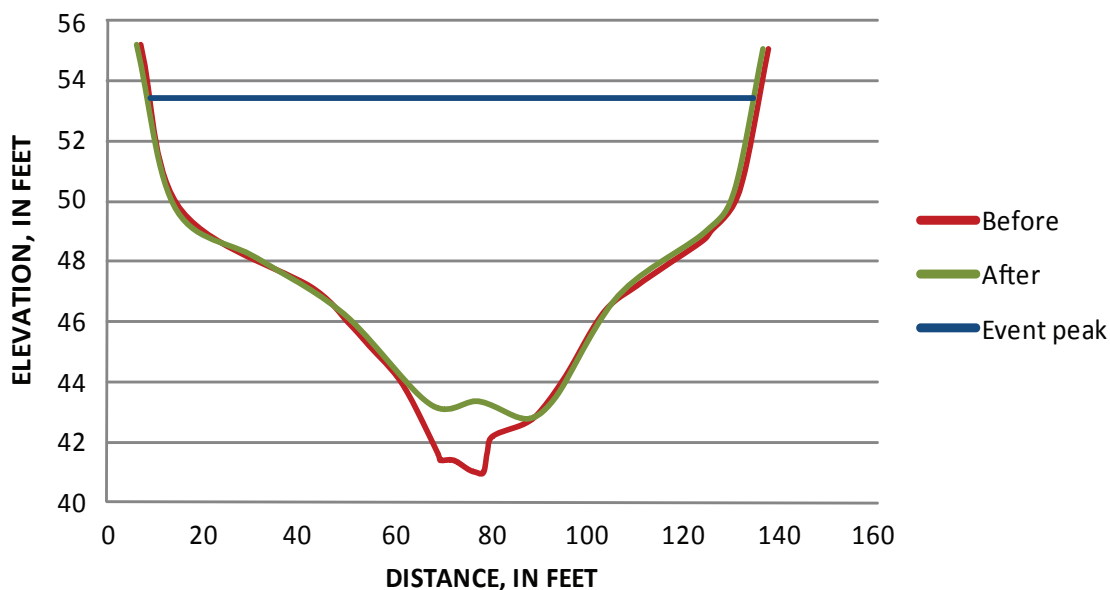


Figure 31. Channel surveys in cross section 4 before and after the July 27, 2006, event. The blue line shows the water-surface elevation at the peak discharge. At the peak discharge, the difference in cross-section areas is 4 percent.

Table 4. Water-surface elevations from surveyed high-water marks and pressure transducers from the July 27, 2006, event.

Pressure transducer	High-water mark found near PT (ft)	Peak recorded by the PT (ft)
PTR1	56.57	56.06
PTL1	N/A	55.60
PTR2	56.71	N/A
PTL2	N/A	55.27
PTR3	55.30	55.08
PTL3	55.79	56.95
PTR4	55.06	54.47
PTL4	55.19	N/A

Table 5. Peak discharge computed using surveyed left-bank high-water marks for the July 27, 2006, event.

Reach	Fall (ft)	Discharge (ft ³ /s)
X3-X4	0.60	12,044

Table 6. Peak discharges computed using surveyed right-bank high-water marks for the July 27, 2006, event.

Reach	Fall (ft)	Discharge (ft ³ /s)
X1-X2	-0.14	NA
X2-X3	1.41	12,409
X3-X4	0.24	7,818
X1-X3	1.27	10,791
X2-X4	1.65	11,230
X1-X4	1.51	10,089

Table 7. Peak discharge computed with the left-bank pressure transducers for the July 27, 2006, event.

Reach	Fall (ft)	Discharge (ft ³ /s)
X1-X2	0.33	8,466

Table 8. Peak discharge computed with the right-bank pressure transducers for the July 27, 2006, event.

Reach	Fall (ft)	Discharge (ft ³ /s)
X1-X3	0.98	9,138
X3-X4	0.61	10,589
X1-X4	1.59	9,621

Stage-discharge relations were developed for the gaging station for conditions before and following the vegetation scour using the stage values from the gaging station with corresponding discharge values that were computed using the CSA method (fig. 37). Travel time between the two locations was small and neglected in developing the rating curves.

Conclusions

The CSA method uses continuously recording pressure transducers to extend slope-area methods for computing peak discharge to entire event hydrographs. The method was initially implemented on the Babocomari River in Arizona in

2002. The pressure transducers provide records of stage that are input to the slope-area SAC program (Fulford, 1994) with cross-section and roughness information to compute discharge hydrographs. The CSA method can produce the event-peak stage and discharge, continuous-discharge hydrographs for an event, and a stage-discharge relation for the site. The SAC program provides considerable flexibility in computing discharge, including the specification of a stage-dependent n .

Discharges calculated with the CSA method are subject to the same error sources as indirect measurements. Surveying errors are typically small, and significant survey errors are usually evident if standard surveying practice is followed. Accuracy of the roughness parameter depends on available information and the judgment of the user, as with any indirect

**Figure 32.** Debris pile near left bank in cross section 3 after the July 27, 2006, event.

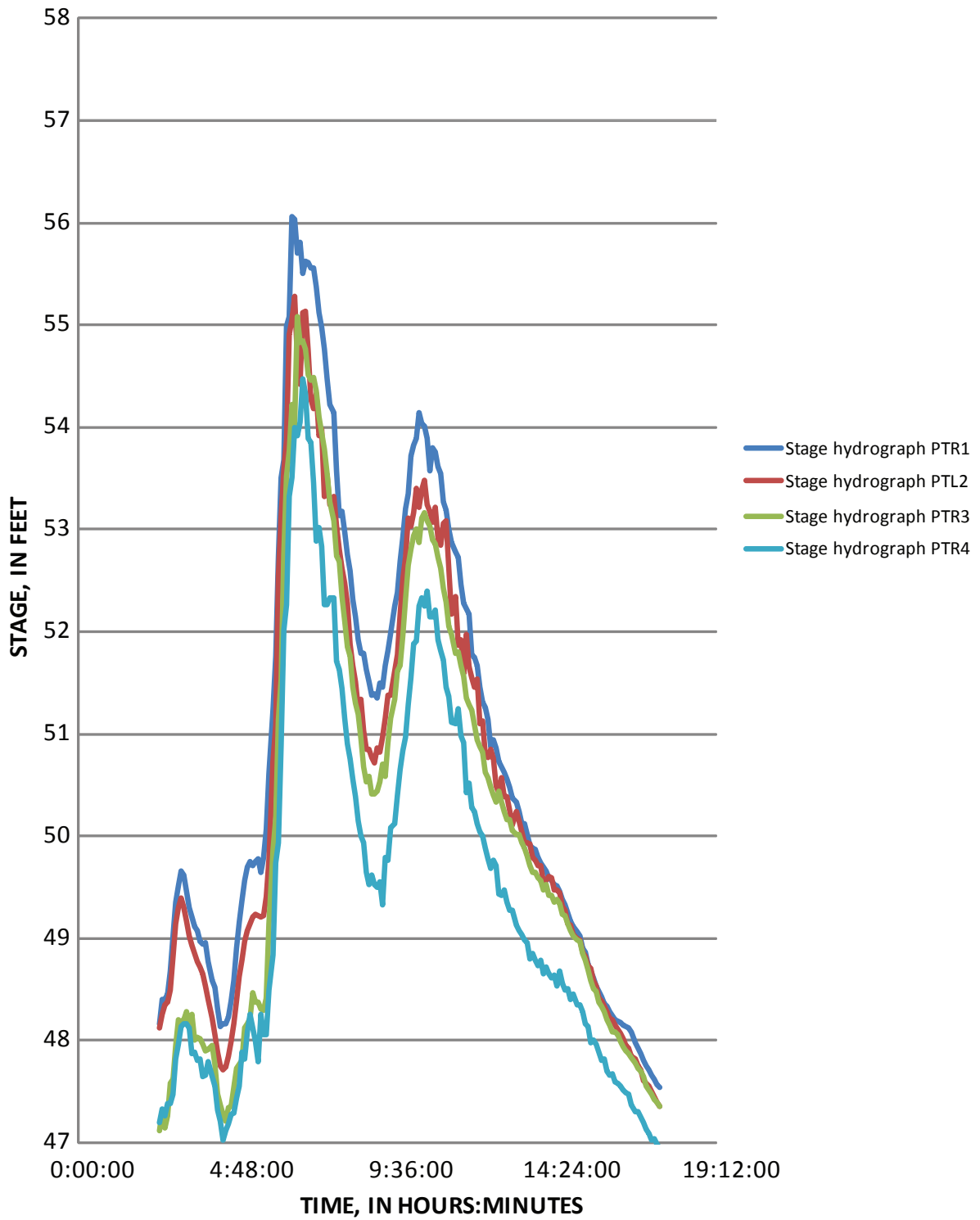


Figure 33. Stage hydrographs of the four pressure transducers that were used to compute discharge for the July 27, 2006, event.

measurement. The CSA method adds more information regarding a flow event but requires a corresponding amount of data evaluation, especially if the flow was sufficient to rearrange the channel or damage instruments. The continuous record of stage at multiple locations offers the opportunity to decipher the short history of a flow event in a way that is not possible with a slope-area method but at the cost of sorting through a larger volume of information.

In the study on the Babocomari River, comparisons to slope-area computations were made by using the high-water marks recorded by the CSGs or high-water marks surveyed in the CSA cross sections. The computed discharge was then compared to a discharge computed using the peak values recorded by the CSA PTs. Only two events are discussed in detail in this report, but similar applications were completed for all the flow events that produced good results. On

occasion, PTs or high-water marks were affected by local conditions, such as debris piles, that degrade the accuracy of computed discharges. The data were not used where this occurred.

Ongoing experiments in CSA applications are refining optimum installation designs of the pressure transducers. The main consideration when installing a PT is stability of the base. The CSG design by Rantz (1982) is excellent at collecting the crest elevations. These types of gages are installed in areas out of the main area of flow that have slower velocities. To collect streamflow data at lower discharges, the PTs need to be installed nearer the deeper parts of the channel in the main areas of flow. The design of the PT installation in the Babocomari River performed well for the medium-flow ranges, as in the first four flow events. At discharges closer to the peak discharge of 9,600 ft³/s, the bases of the CSG gages

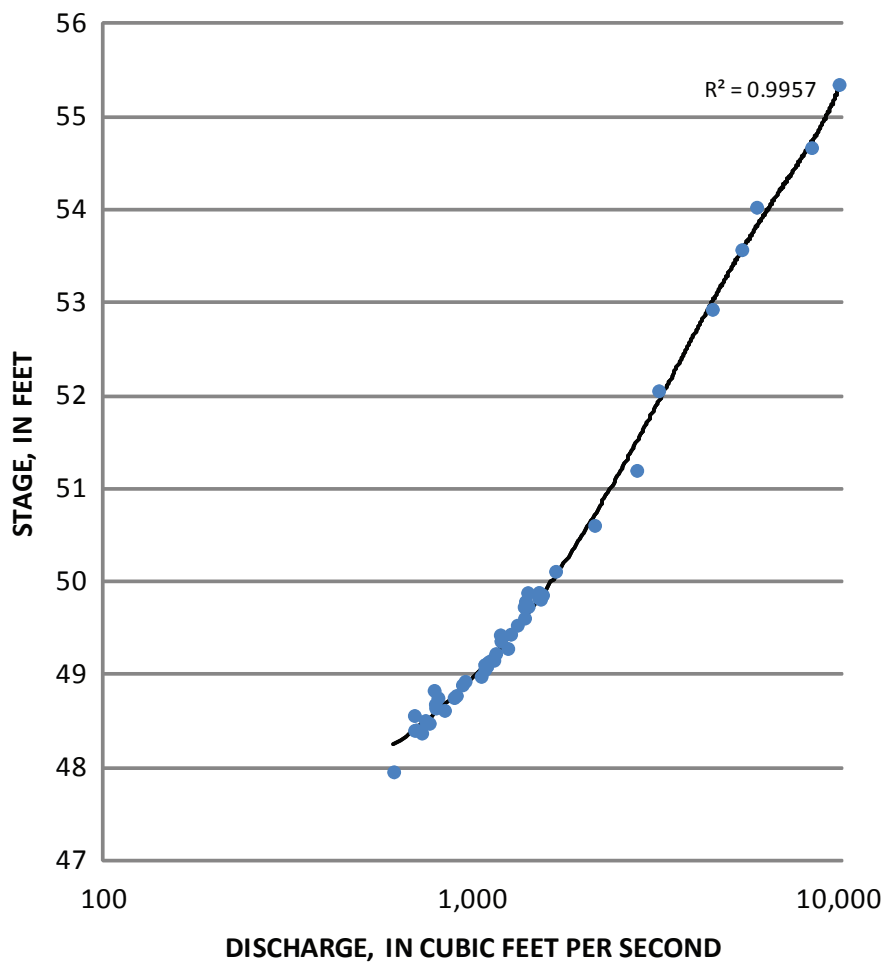


Figure 34. Stage values from the left-bank pressure transducer in cross section 1 and the corresponding discharge computed with stage data in X1-X4 during the July 27, 2006, event are shown as dots. All stage and discharges shown occurred prior to the rotation of the pressure transducers. The solid line is a cubic polynomial fitted to the stage-discharge relation.



Figure 35. Reach below the Babocomari River near the Tombstone stream gage was heavily vegetated prior to the July 27, 2006, event (left). Much of that vegetation was gone after the event (right). The rock in the right foreground of the left photograph is the same as the rock occupying the right lower quadrant of the right photograph.

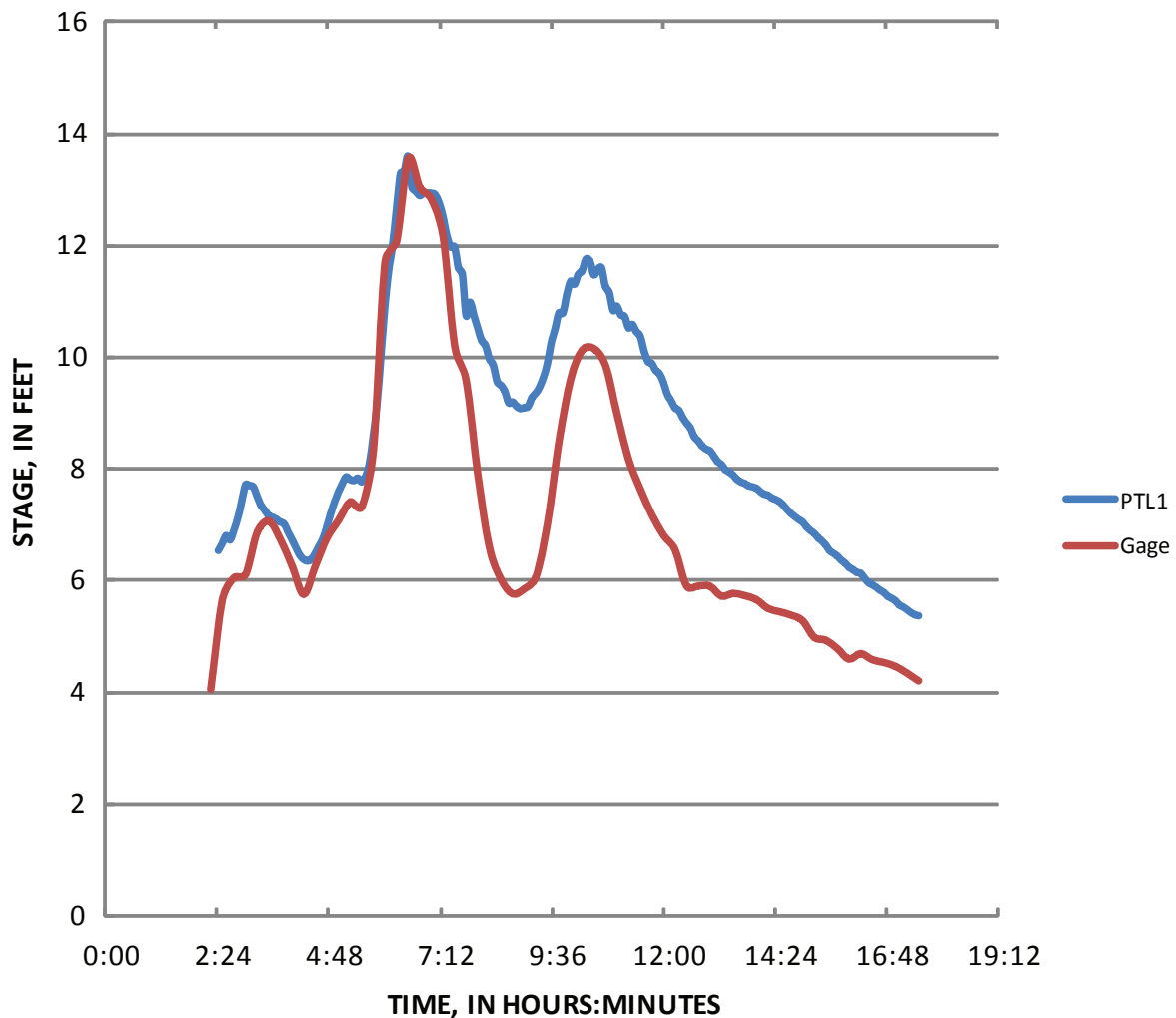


Figure 36. Stage hydrographs from the Babocomari River near Tombstone gage and the left-bank pressure transducer in cross section 1 (PTL1) during the July 27, 2006, event. Stages from the two sites were adjusted to coincide on the rising limb.

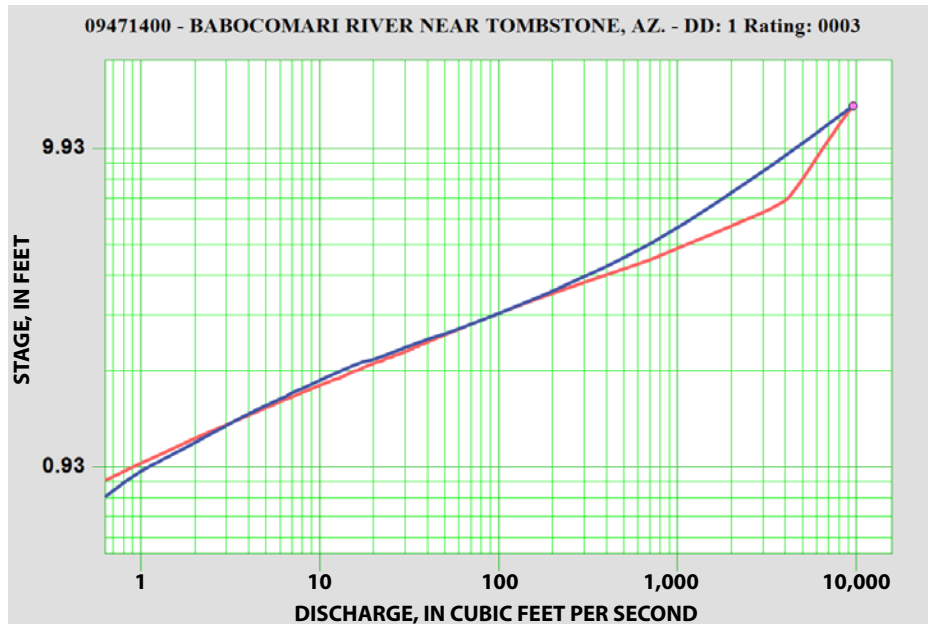


Figure 37. Stage-discharge relations before and after the July 27, 2006, event. The blue line represents conditions prior to the peak and included the effects of the dense vegetation. The red curve represents the condition after vegetation was scoured.

were scoured out, causing the CSA gage to rotate. Future installations of CSA gages should utilize shorter pipes that will collect less debris, and pipes should be angled at 45° to allow them to better shed debris. This design will survive large flows but will lose the ability to record the crest elevation of a flood on the CSGs.

References Cited

- Aldridge, B.N., and Garrett, J.M., 1973, Roughness coefficients for stream channels in Arizona: U.S. Geological Survey Open-File Report 73-3, 87 p.
- Benson, M.A., and Dalrymple, T., 1967, General field and office procedures for indirect discharge measurements: U.S. Geological Survey Techniques of Water-Resources Investigations, book 3, chap. A1, 12 p. (<http://pubs.er.usgs.gov/usgpsubs/twri/twri03A1>).
- Dalrymple, T., and Benson, M.A., 1967, Measurement of peak discharge by the slope-area method: U.S. Geological Survey Techniques of Water-Resources Investigations, book 3, chap. A2, 12 p. (http://pubs.usgs.gov/twri/twri3-a2/pdf/twri_3-A2_a.pdf).
- Fulford, J. M., 1994, User's guide to SAC, a computer program for computing discharge by slope-area method: U.S. Geological Survey Open File Report 94-360, 31 p.
- Phillips, J.V., and Thomas, B.E., 2005, Hydrologic conditions in Arizona during 1999–2004—A historical perspective: U.S. Geological Survey Fact Sheet 2005-3081, 4 p.
- Phillips, J.V., and Tadayon, S., 2006, Selection of Manning's roughness coefficient for natural and constructed vegetated and non-vegetated channels, and vegetation maintenance plan guidelines for vegetated channels in central Arizona: U.S. Geological Survey Scientific Investigations Report 2006-5108, 41 p.
- Pool, D.R., and Coes, A.L., 1999, Hydrogeologic investigations of the Sierra Vista subwatershed of the upper San Pedro Basin, Cochise County, southeast Arizona: U.S. Geological Survey Water-Resources Investigations Report 99-4197, 41 p.
- Rantz, S.E., 1982, Measurement and computation of streamflow, Volume 1—Measurement of stage and discharge: U.S. Geological Water-Supply Paper 2175, 284 p.
- Stewart, A. M., Callegary, J.B., Smith, C.F., Wiele, S.M., Cordova, J.T., Fritzinger, R.A., and Gupta, H.V., 2008, Use of the Continuous Slope-Area Method to Estimate Runoff Through Ephemeral Stream Channels in SE Arizona, Eos Trans. AGU 89(53), Fall Meet. Suppl., Abstract H11E-0823.
- Thomsen, B.W., and Hjalmarson, H.W., 1991, Estimated Manning's roughness coefficient for stream channels and flood plains in Maricopa County, Arizona: Phoenix, Flood Control District of Maricopa County report, 126 p.
- Waltemeyer, S.D., 2005, Automated crest-stage gage application in ephemeral streams in New Mexico: U.S. Geological Survey Fact Sheet 2005-3136, 4 p.
- Wiele, S.M. and Smith, J.D., 1996, A reach-averaged model of diurnal discharge wave propagation down the Colorado River through the Grand Canyon: Water Resources Research, v. 32, no. 5, p. 1375–1386.

Appendix 1. Stage data and computed discharge for five runoff events in the Babocomari River.

August 3, 2002 runoff event on the Babocomari River

Date and time	Right Bank				Date and time	Left Bank			
	Stage, in feet					Stage, in feet			
	PTR1	PTR2	PTR3	PTR4		PTL1	PTL2	PTL3	PTL4
8/3/02 12:50	46.37	46.19	45.63	45.43	8/3/02 12:50	NA	46.46	45.77	45.31
8/3/02 12:55	46.41	46.20	45.73	45.56	8/3/02 12:55	NA	46.46	45.79	45.41
8/3/02 13:00	46.47	46.35	45.84	45.64	8/3/02 13:00	NA	46.46	45.94	45.52
8/3/02 13:05	46.72	46.61	46.10	45.90	8/3/02 13:05	NA	46.70	46.16	45.78
8/3/02 13:10	46.78	46.72	46.18	45.98	8/3/02 13:10	NA	46.81	46.24	45.86
8/3/02 13:15	46.86	46.88	46.29	46.10	8/3/02 13:15	NA	46.98	46.38	45.97
8/3/02 13:20	47.09	47.00	46.47	46.28	8/3/02 13:20	NA	47.16	46.55	46.15
8/3/02 13:25	47.14	47.16	46.51	46.30	8/3/02 13:25	NA	47.21	46.63	46.19
8/3/02 13:30	47.16	47.11	46.53	46.21	8/3/02 13:30	NA	47.28	46.71	46.21
8/3/02 13:35	47.07	47.04	46.49	46.23	8/3/02 13:35	NA	47.16	46.64	46.17
8/3/02 13:40	46.87	46.79	46.29	46.02	8/3/02 13:40	NA	46.93	46.44	45.97
8/3/02 13:45	46.74	46.63	45.98	45.78	8/3/02 13:45	NA	46.70	46.22	45.66
8/3/02 13:50	46.62	46.39	45.77	45.56	8/3/02 13:50	NA	46.47	45.97	45.45
8/3/02 13:55	46.53	46.29	45.65	45.39	8/3/02 13:55	NA	46.41	45.84	45.33

Note: PTL1 was not inundated

Date and time	Average stage, in feet				Computed discharge, ft ³ /s
	X1	X2	X3	X4	
8/3/02 12:50		46.32	45.70	45.37	431
8/3/02 12:55		46.33	45.76	45.48	428
8/3/02 13:00		46.41	45.89	45.58	458
8/3/02 13:05		46.65	46.13	45.84	528
8/3/02 13:10		46.77	46.21	45.92	566
8/3/02 13:15		46.93	46.33	46.04	620
8/3/02 13:20		47.08	46.51	46.22	675
8/3/02 13:25		47.19	46.57	46.24	724
8/3/02 13:30		47.20	46.62	46.21	750
8/3/02 13:35		47.10	46.56	46.20	702
8/3/02 13:40		46.86	46.37	45.99	620
8/3/02 13:45		46.67	46.10	45.72	551
8/3/02 13:50		46.43	45.87	45.51	471
8/3/02 13:55		46.35	45.74	45.36	447

July 25, 2003 runoff event on the Babocomari River

Date and time	Right bank				Date and time	Left bank			
	Stage, in feet					Stage, in feet			
	PTR1	PTR3	PTR5	PTR7		PTL 2	PTL 4	PTL 6	PTL 8
7/25/03 19:10	46.25	45.73	45.57	44.17	7/25/03 19:10	47.346	46.412	45.74	45.255
7/25/03 19:15	46.92	46.76	46.09	45.80	7/25/03 19:15	47.345	46.766	46.107	45.646
7/25/03 19:20	47.03	46.78	46.06	46.12	7/25/03 19:20	47.343	46.822	46.333	46.017
7/25/03 19:25	46.867	46.67	46.001	45.97	7/25/03 19:25	47.347	46.713	46.219	45.872
7/25/03 19:30	46.674	46.432	45.887	45.683	7/25/03 19:30	47.349	46.522	46.027	45.619
7/25/03 19:35	46.425	46.119	45.573	45.239	7/25/03 19:35	47.352	46.415	45.746	45.289

Date and time	Average stage, in feet				Computed discharge, ft ³ /s
	X1	X2	X3	X4	
7/25/03 19:10	46.80	46.07	45.65	44.71	430
7/25/03 19:15	47.13	46.76	46.10	45.73	527
7/25/03 19:20	47.19	46.80	46.20	46.07	508
7/25/03 19:25	47.11	46.69	46.11	45.92	491
7/25/03 19:30	47.01	46.48	45.96	45.65	468
7/25/03 19:35	46.89	46.27	45.66	45.26	429

October 9, 2003 runoff event on the Babocomari River

Date and time	Right bank				Date and time	Left bank			
	Stage, in feet					Stage, in feet			
	PTR1	PTR2	PTR3	PTR4		PTL 2	PTL 4	PTL 6	CSA8
10/9/03 19:35	46.231	45.657	45.578	44.244	10/9/03 19:35	47.339	46.405	45.727	45.271
10/9/03 19:40	46.817	46.506	46.136	45.599	10/9/03 19:40	47.337	46.549	46.073	45.544
10/9/03 19:45	47.03	46.781	46.349	46.118	10/9/03 19:45	47.339	46.883	46.424	46.062
10/9/03 19:50	47.254	46.907	46.386	46.3	10/9/03 19:50	47.452	47.145	46.636	46.227
10/9/03 19:55	47.297	46.995	46.384	46.338	10/9/03 19:55	47.493	47.103	46.627	46.239
10/9/03 20:00	47.2	46.975	46.296	46.172	10/9/03 20:00	47.369	47.039	46.539	46.122
10/9/03 20:05	47.019	46.693	45.995	45.885	10/9/03 20:05	47.34	46.788	46.333	45.804
10/9/03 20:10	46.766	46.475	45.893	45.481	10/9/03 20:10	47.34	46.442	46.072	45.398
10/9/03 20:15	46.471	46.172	45.655	45.08	10/9/03 20:15	47.34	46.405	45.822	45.284

Date and time	Average stage, in feet				Computed discharge, ft ³ /s
	X1	X2	X3	X4	
10/9/03 19:35	46.231	46.031	45.6525	44.7575	340
10/9/03 19:40	46.817	46.5275	46.1045	45.5715	459
10/9/03 19:45	47.1845	46.832	46.3865	46.09	529
10/9/03 19:50	47.353	47.026	46.511	46.2635	580
10/9/03 19:55	47.395	47.049	46.5055	46.2885	591
10/9/03 20:00	47.2845	47.007	46.4175	46.147	567
10/9/03 20:05	47.1795	46.7405	46.164	45.8445	530
10/9/03 20:10	46.766	46.4585	45.9825	45.4395	444
10/9/03 20:15	46.471	46.2885	45.7385	45.182	374

August 15, 2005 runoff event on the Babocomari River

Minutes	Left bank			Computed discharge, ft ³ /s
	Stage, recorded in feet			
	PTL1	PTR2	PTL3	
0	47.375	47.035	46.332	607
5	47.55	47.159	46.486	664
10	47.499	47.138	46.431	650
15	47.441	47.075	46.381	627
20	47.365	47.013	46.321	602
25	47.569	47.271	46.548	678
30	47.723	47.343	46.685	728
35	47.785	47.465	46.861	746
40	47.818	47.524	46.945	748
45	47.834	47.51	46.891	764
50	47.839	47.471	46.912	759
55	47.824	47.474	46.878	756
60	47.812	47.411	46.85	749
65	47.765	47.409	46.835	737
70	47.728	47.372	46.8	720
75	47.66	47.341	46.752	695
80	47.609	47.228	46.689	668
85	47.567	47.15	46.623	653
90	47.492	47.046	46.52	623
95	47.45	46.916	46.46	600
100	47.406	46.826	46.422	580
105	47.39	46.739	46.351	572
110	47.56	47.242	46.611	662
115	47.856	47.684	46.877	801
120	48.06	47.912	47.064	897
125	48.137	47.988	47.205	918
130	48.133	48.008	47.237	909
135	48.134	48.014	47.278	900
140	48.093	47.969	47.25	879
145	48.025	47.955	47.187	857
150	47.958	47.808	47.105	823
155	47.856	47.661	47.021	770
160	47.846	47.534	46.895	772
165	47.747	47.549	46.823	749
170	47.697	47.415	46.736	723
175	47.629	47.303	46.671	690
180	47.575	47.226	46.608	667
185	47.516	47.174	46.526	648
190	47.459	47.045	46.512	613
195	47.406	46.899	46.488	578

July 27, 2006 runoff event on the Babocomari River

Time	Stage, recorded in feet				Discharge, in cfs
	PTR1	PTL2	PTR3	PTR4	CSA Discharge
2:15:00	46.726	46.479	45.633	44.333	383
2:20:00	47.664	47.486	46.888	46.356	645
2:25:00	48.164	48.12	47.122	47.202	706
2:30:00	48.398	48.252	47.298	47.334	807
2:35:00	48.399	48.346	47.138	47.258	806
2:40:00	48.459	48.373	47.264	47.379	821
2:45:00	48.675	48.497	47.575	47.381	981
2:50:00	49.023	48.806	47.623	47.478	1,139
2:55:00	49.352	49.146	47.954	47.824	1,311
3:00:00	49.507	49.307	48.203	47.969	1,427
3:05:00	49.663	49.393	48.181	48.132	1,455
3:10:00	49.619	49.305	48.208	48.157	1,423
3:15:00	49.465	49.165	48.287	48.162	1,352
3:20:00	49.301	49.021	48.134	48.128	1,216
3:25:00	49.208	48.927	48.249	47.867	1,281
3:30:00	49.109	48.853	48.002	47.887	1,155
3:35:00	49.078	48.775	48.033	47.8	1,171
3:40:00	48.976	48.724	48.013	47.819	1,103
3:45:00	48.944	48.647	47.958	47.652	1,121
3:50:00	48.963	48.535	47.899	47.664	1,103
3:55:00	48.77	48.404	47.912	47.787	949
4:00:00	48.59	48.21	47.953	47.641	891
4:05:00	48.516	48.056	47.767	47.559	839
4:10:00	48.308	47.881	47.478	47.314	768
4:15:00	48.141	47.75	47.372	47.204	700
4:20:00	48.161	47.711	47.273	47.027	739
4:25:00	48.163	47.746	47.21	47.114	712
4:30:00	48.235	47.847	47.343	47.181	753
4:35:00	48.386	47.997	47.355	47.274	806
4:40:00	48.584	48.166	47.536	47.296	925
4:45:00	48.899	48.392	47.73	47.431	1,088
4:50:00	49.156	48.626	47.767	47.558	1,196
4:55:00	49.363	48.778	47.803	47.89	1,218
5:00:00	49.56	48.966	48.123	47.816	1,435
5:05:00	49.692	49.073	48.169	48.088	1,445
5:10:00	49.749	49.142	48.215	48.257	1,443
5:15:00	49.715	49.212	48.464	48.121	1,558
5:20:00	49.749	49.233	48.375	47.991	1,585
5:25:00	49.771	49.222	48.376	47.787	1,641
5:30:00	49.64	49.21	48.308	48.249	1,423
5:35:00	49.785	49.225	48.293	48.06	1,557
5:40:00	50.072	49.403	48.409	48.058	1,743
5:45:00	50.611	49.775	49.138	48.498	2,224
5:50:00	51.245	50.732	49.866	48.834	2,988
5:55:00	51.755	51.082	50.172	49.742	3,302
6:00:00	52.724	52.546	51.135	49.933	4,749
6:05:00	53.509	53.121	51.53	50.889	5,546
6:10:00	53.678	53.581	52.752	52.018	6,020
6:15:00	54.986	53.877	53.522	52.261	8,481
6:25:00	56.055	55.055	54.226	53.507	10,097

Appendix 2. Input files to the SAC program used in the continuous slope-area calculations of discharge for five events on the Babocomari river. These files are templates. The stages are replaced when computing the hydrograph with stages from the CSA pressure transducers. Documentation of the SAC program can be found in Fulford (1994).

T1 Babocomari River CSA reach
T2 08/03/2002 event
 XS X4 0.0
 GR 0.0,48.1 11.8,47.1 18.8,46.0 23.3,45.2 30.3,43.9 37.6,41.6
 GR 38.0,41.4 40.8,41.4 43.8,41.1 45.4,41.0 47.0,41.0 47.8,41.7
 GR 48.9,42.2 55.3,42.6 58.6,43.0 64.0,44.2 71.8,46.3 78.8,47.2
 GR 84.2,47.8 92.5,48.7
 N 0.035
 HP X4 46.12
 XS X3 111
 GR 0.0,48.1 3.8,47.4 12.4,46.5 18.8,45.7 30.9,43.7 35.5,43.2
 GR 37.5,42.2 37.9,41.5 43.8,41.3 44.5,42.6 48.7,43.7 53.9,44.6
 GR 59.6,45.3 62.1,45.4 67.4,47.2 75.5,48.4 79.7,49.9
 N 0.035
 HP X3 46.06
 XS X2 190
 GR 0.0,49.4 6.6,48.1 10.4,47.5 15.1,47.1 21.1,46.1 30.1,45.5
 GR 33.9,44.8 36.2,43.6 37.2,41.4 47.5,41.8 48.2,42.7 51.5,44.1
 GR 55.2,44.7 59.7,45.5 66.9,46.5 70.7,47.2 74.9,48.1 86.2,51.6
 GR 92.1,52.5
 N 0.035
 HP X2 46.78
 XS X1 300
 GR 0.56.6 6.3,52.8 8.1,49.6 15.8,48.4 22.1,48 23.5,47.4 30.7,46.6
 GR 35.9,45.6 39.7,45.3 43.1,44.8 49.2,44.2 54.4,44 55.8,42.6 58.1,42.8
 GR 58.8,44 61.6,44.4 64.5,45.3 67.2,45.6 70.5,45.8 75,46.8 81.2,47.9
 GR 84,48.4 96.9,52.8 100.5,54.4
 N 0.035
 HP X1 47.03

T1 Babocomari River CSA reach
T2 07/25/2003 event
 XS X4 0.0
 GR 0.0,48.1 11.8,47.1 18.8,46.0 23.3,45.2 30.3,43.9 37.6,41.6
 GR 38.0,41.4 40.8,41.4 43.8,41.1 45.4,41.0 47.0,41.0 47.8,41.7
 GR 48.9,42.2 55.3,42.6 58.6,43.0 64.0,44.2 71.8,46.3 78.8,47.2
 GR 84.2,47.8 92.5,48.7
 N 0.035
 HP X4 46.12
 XS X3 111
 GR 0.0,48.1 3.8,47.4 12.4,46.5 18.8,45.7 30.9,43.7 35.5,43.2
 GR 37.5,42.2 37.9,41.5 43.8,41.3 44.5,42.6 48.7,43.7 53.9,44.6
 GR 59.6,45.3 62.1,45.4 67.4,47.2 75.5,48.4 79.7,49.9
 N 0.035
 HP X3 46.06
 XS X2 190
 GR 0.0,49.4 6.6,48.1 10.4,47.5 15.1,47.1 21.1,46.1 30.1,45.5
 GR 33.9,44.8 36.2,43.6 37.2,41.4 47.5,41.8 48.2,42.7 51.5,44.1
 GR 55.2,44.7 59.7,45.5 66.9,46.5 70.7,47.2 74.9,48.1 86.2,51.6
 GR 92.1,52.5
 N 0.035
 HP X2 46.78
 XS X1 300
 GR 0.56.6 6.3,52.8 8.1,49.6 15.8,48.4 22.1,48 23.5,47.4 30.7,46.6
 GR 35.9,45.6 39.7,45.3 43.1,44.8 49.2,44.2 54.4,44 55.8,42.6 58.1,42.8
 GR 58.8,44 61.6,44.4 64.5,45.3 67.2,45.6 70.5,45.8 75,46.8 81.2,47.9
 GR 84,48.4 96.9,52.8 100.5,54.4
 N 0.035
 HP X1 47.03

36 The Continuous Slope-Area Method for Computing Event Hydrographs

T1 Babocamari River CSA reach

T2 10/09/2003 event

XS X4 0.0
GR 0.0,48.1 11.8,47.1 18.8,46.0 23.3,45.2 30.3,43.9 37.6,41.6
GR 38.0,41.4 40.8,41.4 43.8,41.1 45.4,41.0 47.0,41.0 47.8,41.7
GR 48.9,42.2 55.3,42.6 58.6,43.0 64.0,44.2 71.8,46.3 78.8,47.2
GR 84.2,47.8 92.5,48.7
N 0.035
HP X4 46.09
XS X3 111
GR 0.0,48.1 3.8,47.4 12.4,46.5 18.8,45.7 30.9,43.7 35.5,43.2
GR 37.5,42.2 37.9,41.5 43.8,41.3 44.5,42.6 48.7,43.7 53.9,44.6
GR 59.6,45.3 62.1,45.4 67.4,47.2 75.5,48.4 79.7,49.9
N 0.035
HP X3 46.39
XS X2 190
GR 0.0,49.4 6.6,48.1 10.4,47.5 15.1,47.1 21.1,46.1 30.1,45.5
GR 33.9,44.8 36.2,43.6 37.2,41.4 47.5,41.8 48.2,42.7 51.5,44.1
GR 55.2,44.7 59.7,45.5 66.9,46.5 70.7,47.2 74.9,48.1 86.2,51.6
GR 92.1,52.5
N 0.035
HP X2 46.83
XS X1 300
GR 0.56,6 6.3,52 8.1,49.6 15.8,48.4 22.1,48 23.5,47.4 30.7,46.6
GR 35.9,45.6 39.7,45.3 43.1,44.8 49.2,44.2 54.4,44 55.8,42.6 58.1,42.8
GR 58.8,44 61.6,44.4 64.5,45.3 67.2,45.6 70.5,45.8 75.46,8 81.2,47.9
GR 84.48,4 96.9,52.8 100.5,54.4
N 0.035
HP X1 47.18

T1 Babocamari River CSA reach

T2 8/15/2005 event

XS X4 0.0
GR 006.00,055.19 014.00,049.78 041.80,047.10 048.80,046.00
GR 053.30,045.20 060.30,043.90 067.60,041.60 068.00,041.40
GR 070.80,041.40 073.80,041.10 075.40,041.00 077.00,041.00
GR 077.80,041.70 078.90,042.20 085.30,042.60 088.60,043.00
GR 094.00,044.20 101.80,046.30 108.80,047.20 114.20,047.80
GR 122.50,048.70 124.00,048.99 130.00,050.33 136.00,055.06
N 0.035
HP X4 44.333
XS X3 115
GR 003.00,055.79 019.80,048.30 031.50,046.60 035.70,046.30
GR 038.70,045.80 042.20,045.20 047.20,044.50 050.50,043.90
GR 053.30,043.50 055.30,043.70 056.20,043.10 059.50,041.00
GR 061.10,040.90 063.10,041.00 064.50,041.70 065.40,043.00
GR 066.80,043.60 070.90,043.90 074.50,044.60 075.80,044.50
GR 077.10,044.70 078.40,045.00 081.90,045.40 083.10,046.10
GR 086.60,046.80 091.00,047.60 101.00,050.28 106.10,050.80
GR 120.00,052.69 138.00,055.30
N 0.035
HP X3 45.633
XS X2 188
GR 001.70,055.50 003.00,054.83 006.00,053.06 012.60,050.62
GR 017.20,049.42 022.00,048.97 028.50,048.16 043.50,045.77
GR 044.00,046.35 052.00,045.57 056.50,043.97 056.50,041.47
GR 066.00,041.77 070.00,042.07 070.50,043.07 077.00,045.17
GR 077.50,045.58 085.00,046.27 095.00,048.09 098.00,048.82
GR 098.00,048.82 101.00,049.75 107.70,052.00 115.80,053.37
GR 126.40,054.23 136.20,055.41 139.00,056.71
N 0.035
HP X2 46.479
XS X1 301
GR 004.00,058.65 019.00,050.48 027.60,049.00 031.10,048.00
GR 034.30,047.70 036.00,047.90 037.50,047.50 038.90,047.30
GR 041.40,046.80 042.20,046.80 044.80,046.50 049.90,045.70
GR 055.00,045.27 057.30,044.80 061.90,044.60 067.90,044.10
GR 068.40,042.80 069.60,042.70 070.10,043.10 070.70,042.80
GR 071.00,042.60 071.40,042.70 071.80,043.80 074.80,044.50
GR 078.20,045.40 079.50,045.50 082.00,045.60 082.90,045.50
GR 084.30,045.80 088.00,046.70 091.70,047.20 098.70,048.60
GR 099.00,048.80 107.00,052.16 116.00,054.82 128.00,056.57
N 0.035
HP X1 46.726

T1 Babocomari River CSA reach
T2 7/27/2006 event
 XS X4 0.0
 GR 006.00,055.19 014.00,049.78 041.80,047.10 048.80,046.00
 GR 053.30,045.20 060.30,043.90 067.60,041.60 068.00,041.40
 GR 070.80,041.40 073.80,041.10 075.40,041.00 077.00,041.00
 GR 077.80,041.70 078.90,042.20 085.30,042.60 088.60,043.00
 GR 094.00,044.20 101.80,046.30 108.80,047.20 114.20,047.80
 GR 122.50,048.70 124.00,048.99 130.00,050.33 136.00,055.06
 N 0.040
 HP X4 44.333
 XS X3 115
 GR 003.00,055.79 019.80,048.30 031.50,046.60 035.70,046.30
 GR 038.70,045.80 042.20,045.20 047.20,044.50 050.50,043.90
 GR 053.30,043.50 055.30,043.70 056.20,043.10 059.50,041.00
 GR 061.10,040.90 063.10,041.00 064.50,041.70 065.40,043.00
 GR 066.80,043.60 070.90,043.90 074.50,044.60 075.80,044.50
 GR 077.10,044.70 078.40,045.00 081.90,045.40 083.10,046.10
 GR 086.60,046.80 091.00,047.60 101.00,050.28 106.10,050.80
 GR 120.00,052.69 138.00,055.30
 N 0.040
 HP X3 45.633
 XS X2 188
 GR 001.70,055.50 003.00,054.83 006.00,053.06 012.60,050.62
 GR 017.20,049.42 022.00,048.97 028.50,048.16 043.50,045.77
 GR 044.00,046.35 052.00,045.57 056.50,043.97 056.50,041.47
 GR 066.00,041.77 070.00,042.07 070.50,043.07 077.00,045.17
 GR 077.50,045.58 085.00,046.27 095.00,048.09 098.00,048.82
 GR 098.00,048.82 101.00,049.75 107.70,052.00 115.80,053.37
 GR 126.40,054.23 136.20,055.41 139.00,056.71
 N 0.040
 HP X2 46.479
 XS X1 301
 GR 004.00,058.65 019.00,050.48 027.60,049.00 031.10,048.00
 GR 034.30,047.70 036.00,047.90 037.50,047.50 038.90,047.30
 GR 041.40,046.80 042.20,046.80 044.80,046.50 049.90,045.70
 GR 055.00,045.27 057.30,044.80 061.90,044.60 067.90,044.10
 GR 068.40,042.80 069.60,042.70 070.10,043.10 070.70,042.80
 GR 071.00,042.60 071.40,042.70 071.80,043.80 074.80,044.50
 GR 078.20,045.40 079.50,045.50 082.00,045.60 082.90,045.50

This page intentionally left blank

Produced in the Western Region, Menlo Park, California
Manuscript approved for publication, August 9, 2010
Layout and design by Stephen L. Scott

